

SUPERCONDUCTING QUBITS II: DECOHERENCE

F.K. Wilhelm[†], M.J. Storcz and U. Hartmann

Department Physik, Center for Nanoscience, and Arnold Sommerfeld Center for theoretical physics, Ludwig-Maximilians-Universität, 80333 München, Germany

Michael R. Geller[‡]

Department of Physics, University of Georgia, Athens, Georgia 30602, USA

Abstract. This is an introduction to elementary decoherence theory as it is typically applied to superconducting qubits.

Abbreviations: SQUID – superconducting quantum interference device; qubit – quantum bit; TSS – two state system

Contents

1	Introduction	1
2	Single qubit decoherence	11
3	Beyond Bloch-Redfield	25
4	Decoherence in coupled qubits	34
5	Summary	36
6	Acknowledgements	36

1. Introduction

The transition from quantum to classical physics, now known as decoherence, has intrigued physicists since the formulation of quantum mechanics (Giulini et al., 1996; Leggett, 2002; Peres, 1993; Feynman and Vernon, 1963; Zurek, 1993). It has been put into the poignant Schrödinger cat paradox (Schrödinger, 1935) and was considered an open fundamental question for a long time.

[†] present address: Physics Department and Insitute for Quantum Computing, University of Waterloo, Waterloo, Ontario N2L 3G1, Canada; fwilhelm@iqc.ca

[‡] mgeller@uga.edu



In this chapter, we study the theory of decoherence as it is applied to superconducting qubits. The foundations of the methodology used are rather general results of quantum statistical physics and resemble those applied to chemical physics, nuclear magnetic resonance, optics, and other condensed matter systems (Weiss, 1999). All these realizations introduce their subtleties — typical couplings, temperatures, properties of the correlation functions. We will in the following largely stick to effective spin notation in order to emphasize this universality, still taking most of the examples from superconducting decoherence. This paper is based on lectures 2 and 3 of the NATO-ASI on “Manipulating quantum coherence in superconductors and semiconductors” in Cluj-Napoca, Romania, 2005. It is *not* intended to be a review summarizing the main papers in the field. Rather, it is an (almost) self-contained introduction to some of the relevant techniques, aimed to be accessible to researchers and graduate students with a knowledge of quantum mechanics (Cohen-Tannoudji et al., 1992) and statistical physics (Landau and Lifshitz, 1984) on the level of a first graduate course. So much of the material here is not new and most certainly known to more experienced researchers, however, we felt a lack of a single reference which allows newcomers to get started without excessive overhead. References have largely been chosen for the aid they provide in learning and teaching the subject, rather than importance and achievement.

1.1. BASIC NOTIONS OF DECOHERENCE

The mechanisms of decoherence are usually related to those of energy dissipation. In particular, decoherence is irreversible. If we take as an example a pure superposition state

$$|\psi\rangle = (|0\rangle + |1\rangle)/\sqrt{2} \quad \rho_{\text{pure}} = |\psi\rangle\langle\psi| = \frac{1}{2} \begin{pmatrix} 1 & 1 \\ 1 & 1 \end{pmatrix} \quad (1)$$

and compare it to the corresponding classical mixture leading to the same expectation value of σ_z

$$\rho_{\text{mix}} = \frac{1}{2} \begin{pmatrix} 1 & 0 \\ 0 & 1 \end{pmatrix} \quad (2)$$

we can see that the von-Neumann entropy $\rho = -k_B \text{Tr}[\rho \log \rho]$ rises from $S_{\text{pure}} = 0$ to $S_{\text{mix}} = k_B \ln 2$. Hence, decoherence taking ρ_{pure} to ρ_{mix} creates entropy and is irreversible.

Quantum mechanics, on the other hand, is always reversible. It can be shown, that any *isolated* quantum system is described by the Liouville von-Neumann equation

$$i\hbar\dot{\rho} = [H, \rho] \quad (3)$$

which conserves entropy. Indeed, also the CPT theorem of relativistic quantum mechanics (Sakurai, 1967) states, that for each quantum system it is possible to find a counterpart (with inversed parity and charge) whose time arrow runs backwards. The apparent contradiction between microreversibility — reversibility of the laws of quantum physics described by Schrödinger's equation — and macro-irreversibility is a problem at the foundation of statistical thermodynamics. We also remark that the Lagrangian formalism (Landau and Lifshitz, 1982) which was used as the starting point in the previous chapter of this book (Geller et al., 2006) does not even accomodate friction on a classical level without artificial and in general non-quantizable additions.

1.1.1. *Heat baths and quantum Brownian motion*

The standard way out of this dilemma is to introduce a continuum of additional degrees of freedom acting as a heat bath for the quantum system under consideration (Feynman and Vernon, 1963; Caldeira and Leggett, 1981; Caldeira and Leggett, 1983). The complete system is fully quantum-coherent and can be described by equation 3. However, the heat bath contains unobserved degrees of freedom which have to be integrated out to obtain the *reduced system*; the reduced system is the original quantum system which does not contain the bath explicitly, but whose dynamics are influenced by the bath. The dynamics of the reduced system now show both *dissipation* (energy exchange with the heat bath) and *decoherence* (loss of quantum information to the heat bath). Another view on this is that any finite combined quantum system shows dynamics which are periodic in time. The typical periods are given by the inverse level splittings of the system. Thus, a continuous heat bath shows periodicity and reversibility only on an infinite, physically unobservable time scale.

A standard example, taken from Ref. (Ingold, 1998), of irreversibility in both classical and quantum mechanics is (quantum) Brownian motion (QBM), which we will now describe in the one-dimensional case. The underlying Hamiltonian of a single particle in an oscillator bath has the general structure

$$H = H_s + H_{sb} + H_b + H_c. \quad (4)$$

Here, the system Hamiltonian H_s describes an undamped particle of mass M in a scalar potential, $H_s = \frac{P^2}{2M} + V(q)$. H_b describes a bath of harmonic oscillators, $H_i = \sum_i \left(\frac{p_i^2}{2m_i} + \frac{1}{2}m_i\omega_i^2 x_i^2 \right)$. The coupling between these two components is bilinear, $H_{sb} = -q \sum_i c_i x_i$. If this were all, the effective potential seen by the particle would be altered even on the classical level, as will become more obvious later on. Thus, we have to add a counter term

which does not act on the bath, $H_c = q^2 \sum_i \frac{c_i^2}{2m_i\omega_i^2}$. Adding this counterterm gives the Hamiltonian the following intuitive form

$$H = \frac{P^2}{2M} + V(q) + \sum_i \left(\frac{p_i^2}{2m_i} + \frac{1}{2} m_i \omega_i^2 \left(x_i - \frac{c_i}{m_i \omega_i^2} q \right)^2 \right) \quad (5)$$

indicating that the bath oscillators can be viewed as attached to the particle by springs. Here, we have introduced sets of new parameters, c_i , ω_i , and m_i which need to be adjusted to the system of interest. This aspect will be discussed later on. We treat this system now using the Heisenberg equation of motion

$$i\hbar\dot{O}(t) = [O(t), H] \quad (6)$$

for the operators q , P , x_i , and p_i , which (as a mathematical consequence of the correspondence principle) coincide with the classical equations of motion. The bath oscillators see the qubit acting as an external force

$$\ddot{x}_i + \omega_i^2 x_i = \frac{c_i}{m_i} q(t). \quad (7)$$

This equation of motion can be solved by variation of constants, which can be found in textbooks on differential equations such as (Zill, 2000)

$$x_i(t) = x_i(0) \cos \omega_i t + \frac{p_i(0)}{m_i \omega_i} \sin \omega_i t + \frac{c_i^2}{m_i \omega_i^2} \int_0^t dt' \sin \omega_i(t-t') q(t') \quad (8)$$

Analogously, we find the equation of motion for the particle

$$\ddot{q} = -\frac{\partial V}{\partial q} - \sum \frac{c_i}{m_i} x_i - q \sum \frac{c_i^2}{m_i \omega_i^2}. \quad (9)$$

Substituting eq. 8 into eq. 9 eliminates the bath coordinates up to the initial condition

$$\begin{aligned} M\ddot{q} = & -\frac{\partial V}{\partial q} - \sum_i \frac{c_i^2}{m_i \omega_i} \int_0^t dt' \sin \omega_i(t-t') q(t') \\ & + \sum_i c_i \left(x_i(0) \cos \omega_i t + \frac{p_i(0)}{m_i \omega_i} \sin \omega_i t \right) - q \sum_i \frac{c_i^2}{m_i \omega_i^2}. \end{aligned} \quad (10)$$

We now integrate by parts and get a convolution of the velocity plus boundary terms, one of which shifts the origin of the initial position, the other cancels the counterterm (indicating, that without the counterterm we would obtain a potential renormalization). The result has the compact form

$$M\ddot{q} + \frac{\partial V}{\partial q} + \int_0^t dt' \gamma(t-t') \dot{q}(t') = \xi(t). \quad (11)$$

This structure is identified as a Langevin equation with memory friction. If interpreted classically, this is the equation of motion of a Brownian particle - a light particle in a fluctuating medium. In the quantum limit, we have to read q, x_i and the derived quantity ξ as operators. We see both sides of open system dynamics — Dissipation encoded in the damping kernel γ and decoherence encoded in the noise term ξ . We can express γ as

$$\gamma(t) = \sum_i \frac{c_i^2}{m_i \omega_i^2} \cos \omega_i t = \int_0^\infty \frac{d\omega}{\omega} J(\omega) \cos \omega t \quad (12)$$

where we have introduced the spectral density of bath modes

$$J(\omega) = \sum_i \frac{c_i^2}{m_i \omega_i} \delta(\omega - \omega_i) \quad (13)$$

which is the only quantifier necessary to describe the information encoded in the distribution of the m_i, ω_i , and c_i . The right hand side of eq. 11 is a noise term and reads

$$\xi(t) = \sum_i c_i \left[\left(x_i(0) - \frac{c_i}{m_i \omega_i^2} q(0) \right) \cos \omega_i t + \frac{p_i(0)}{m_i \omega_i} \sin \omega_i t \right]. \quad (14)$$

This crucially depends on the initial condition of the bath. If we assume that the bath is initially equilibrated around the initial position $q(0)$ of the particle, we can show, using the standard quantum-statistics of the simple harmonic oscillator, that the noise is unbiased, $\langle \xi(t) \rangle = 0$, and its correlation function is given by

$$K(t) = \langle \xi(t) \xi(0) \rangle = \int d\omega J(\omega) [\cos \omega t (2n(\hbar\omega) + 1) - i \sin \omega t] \quad (15)$$

where n is the Bose function, $n(\hbar\omega) = (e^{\hbar\omega/kT} - 1)^{-1}$, and $2n(\hbar\omega) + 1 = \coth\left(\frac{\hbar\omega}{2k_B T}\right)$. Here and henceforth, angular brackets around an operator indicate the quantum-statistical average, $\langle O \rangle = \text{Tr}(\rho O)$ with ρ being the appropriate density matrix. We will get back to the topic of the initial condition in section 3.1.2 of this chapter.

The noise described by $\xi(t)$ is the *quantum* noise of the bath. In particular, the correlation function is time-translation invariant,

$$K(t) = \langle \xi(t + \tau) \xi(\tau) \rangle \quad (16)$$

but not symmetric

$$K(-t) = \langle \xi(0) \xi(t) \rangle = K^*(t) \neq K(t). \quad (17)$$

which reflects the fact that ξ as defined in eq. 14 is a time-dependent operator which does generally not commute at two different times. Explicitly, the imaginary part of $K(t)$ changes its sign under time reversal. Indeed, if the derivation of eq. 15 is done explicitly, one directly sees that it originates from the finite commutator. Moreover, we can observe that at $T \gg \omega$ we have $2n + 1 \rightarrow 2k_B T / \hbar \omega \gg 1$, thus the integral in eq. 15 is dominated by the symmetric real part now describing purely thermal noise. At any temperature, the symmetrized semiclassical spectral noise power in frequency space reads

$$S(\omega) = \frac{1}{2} \langle \xi(t)\xi(0) + \xi(0)\xi(t) \rangle_\omega = S(-\omega) \quad (18)$$

where $\langle \dots \rangle_\omega$ means averaging and Fourier transforming. This quantity contains a sign of the quantum nature of noise. Unlike classical noise, it does not disappear at low temperatures $T \ll \hbar \omega / k_B$, but saturates to a finite value set by the zero-point fluctuations, whereas at high temperature we recover thermal noise. Note, that the same crossover temperature dictates the asymmetry in eq. (17). Both observations together can be identified with the fact, that zero-point fluctuations only allow for emission of energy, not absorption, as will be detailed in a later section of this chapter.

Our approach in this chapter is phenomenological. The main parameter of our model is the spectral density $J(\omega)$. We will show in sections 1.1.3, 2.1.1 and 2.1.2 how $J(\omega)$ can be derived explicitly for Josephson junction circuits. Oscillator baths accurately model numerous other situations. Decoherence induced by phonons in quantum dot systems allows to directly identify the phonons as the bath oscillators (Brandes and Kramer, 1999; Storz et al., 2005a), whereas in the case of electric noise from resistors or cotunneling in dots (Hartmann and Wilhelm, 2004) it is less obvious — the Bosons are electron-hole excitations, which turn out to have the commutation relation of hard-core bosons (von Delft and Schoeller, 1998) with the hard-core term being of little effect in the limits of interest (Weiss, 1999).

Going back to our phenomenology, we introduce the most important case of an Ohmic bath

$$J(\omega) = \gamma \omega f(\omega/\omega_c). \quad (19)$$

Here, γ is a constant of dimension frequency and f is a high-frequency cutoff function providing $f(x) \simeq 1$ at $x < 1$ and $f \rightarrow 0$ at $x > 1$. Popular choices include the hard cutoff, $f(x) = \theta(1 - x)$, exponential cutoff, $f(x) = e^{-x}$, and the Drude cutoff $f(x) = \frac{1}{1+x^2}$. We will see in section 1.1.3 that the Drude cutoff plays a significant role in finite electrical circuits, so we chose it here for illustration purposes. In this case, the damping kernel reduces

to

$$\gamma(\tau) = \gamma\omega_c e^{-\omega_c\tau}. \quad (20)$$

For $\omega_c \rightarrow \infty$, γ becomes a delta function and we recover the classical damping with damping constant γ , $\gamma(\tau) = \gamma\delta(\tau)$. Here, “classical damping” alludes to the damping of particle motion in fluid or of charge transport in a resistor (thus the name Ohmic, see also section 1.1.3). With finite ω_c , the Ohmic model leads to classical, linear friction proportional to the velocity, smeared out over a memory time set by the inverse cutoff frequency defining a correlation time $t_c = \omega_c^{-1}$. On the other hand, as it turns out in the analysis of the model e.g. in section 2.2.2, an infinite cutoff always leads to unphysical divergencies. Examples will be given later on. All examples from the class of superconducting qubits have a natural ultraviolet cutoff set by an appropriate $1/RC$ or R/L with R , L , and C being characteristic resistances, inductances, and capacitances of the circuit, respectively. Note, that parts of the open quantum systems literature do not make this last observation.

We will not dwell on methods of solution of the quantum Langevin equation, as the focus of this work is the decoherence of qubit systems. Methods include the associated Fokker-Planck equation, path integrals, and quantum trajectory simulations. The quantum Langevin equation finds application in the theory of quantum decay in chemical reactions, the dissipative harmonic oscillator, and the decoherence of double-slit experiments.

1.1.2. *How general are oscillator baths?*

Even though the model introduced looks quite artificial and specific, it applies to a broad range of systems. The model essentially applies as long as the heat bath can be treated within linear response theory, meaning that it is essentially infinite (i.e. cannot be exhausted), has a regular spectrum, and is in thermal equilibrium. We outline the requirement of only weakly perturbing the system, i.e. of linear response theory (Kubo et al., 1991). The derivation is rather sketchy and just states the main results because this methodology will not be directly used later on. Introductions can be found e.g. in Ref. (Kubo et al., 1991; Ingold, 1998; Callen and Welton, 1951)

In linear response theory, we start from a Hamiltonian H_0 of the oscillator bath which is perturbed by an external force F coupling to a bath operator Q ,

$$H = H_0 - FQ \quad (21)$$

where the perturbation must be weak enough to be treated to lowest order. It is a result of linear response theory that the system responds by a shift

of Q (taken in the Heisenberg picture) according to

$$\langle \delta Q(t) \rangle_\omega = \chi(\omega) F(\omega) \quad (22)$$

where the susceptibility χ can be computed to lowest order as the correlation function

$$\chi = \langle Q(0)Q(0)\theta(t) \rangle_\omega \quad (23)$$

computed in thermal equilibrium. We can split the correlation function into real and imaginary parts $\chi = \chi' + i\chi''$. The real part determines the fluctuations, i.e.

$$\frac{1}{2} \langle \delta Q(t)\delta Q(0) + \delta Q(0)\delta Q(t) \rangle_\omega = \chi' \quad (24)$$

whereas the imaginary part determines the energy dissipation

$$\langle E(t) \rangle_\omega = \omega \chi'' |F|^2. \quad (25)$$

together with the equations 12 and 18 tracing both damping and noise back to a single function χ constitute the famous fluctuation-dissipation theorem (Callen and Welton, 1951), a generalization of the Einstein relation in diffusion.

In this very successful approach we have characterized the distribution of the observable Q close to thermal equilibrium by its two-point correlation function alone. This is a manifestation of the fact that its distribution, following the central limit theorem is Gaussian, i.e. can be characterized by two numbers only: mean and standard deviation. Oscillator baths provide exactly these ingredients: by properly choosing $J(\omega)$ they can be fully adjusted to any $\chi(\omega)$, and all higher correlation functions — correlation functions involving more than two operators — can also be expressed through J hence do not contain any independent piece of information.

This underpins the initial statement that oscillator baths can describe a broad range of environments, including those composed of Fermions and not Bosons, such as a resistor. As explained in section 1.1.1, the oscillators are introduced artificially — on purely statistical grounds as a tool to describe fluctuations and response — and can only sometimes be directly identified with a physical entity.

There are still a number of environments where the mapping on an oscillator bath is in general not correct. These include i) baths of uncoupled spins (e.g. nuclear spins), which are not too big and can easily saturate, i.e. explore the full finite capacity of their bounded energy spectrum ii) shot noise, which is not in thermal equilibrium iii) nonlinear electrical circuits such as many Josephson circuits and iv) in most cases $1/f$ noise,

whose microscopic explanation either hints at non-Gaussian (spin-like) or nonequilibrium sources as discussed in section 3.1.3.

1.1.3. Oscillator bath models for Josephson junction devices

We have now learned two approaches to characterize the oscillator bath: through noise, and through friction. We will now apply the characterization by friction to a simple Josephson circuit with Josephson energy E_J , junction capacitance C_J and arbitrary shunt admittance in parallel, all biased by an external current I_B . We are extending the method presented in the previous chapter (Geller et al., 2006) to include the admittance. We start with the elementary case of a constant conductance, $Y(\omega) = G$. The total current splits up into the three elements as

$$I_B = I_c \sin \phi + C \frac{\Phi_0}{2\pi} \ddot{\phi} + G \frac{\Phi_0}{2\pi} \dot{\phi}. \quad (26)$$

Reordering terms, we can cast this into the shape of Newton's equation for a particle with coordinate ϕ .

$$C \left(\frac{\Phi_0}{2\pi} \right)^2 \ddot{\phi} + G \left(\frac{\Phi_0}{2\pi} \right)^2 \dot{\phi} + \frac{\partial V}{\partial \phi} = 0. \quad (27)$$

Here, we have multiplied the equation by another $\Phi_0/2\pi$ to ensure proper dimensions of the potential energy

$$V(\phi) = -I_B \frac{\Phi_0}{2\pi} \phi + E_J (1 - \cos \phi) \quad (28)$$

where we have introduced the Josephson energy $E_J = I_0 \Phi_0 / 2\pi$. This expression can be readily compared to eq. 11. We see that the friction term has no memory, i.e. $\gamma(t) \propto \delta(t)$, and using the results of section 1.1.1 we can infer that $J(\omega) = G(\Phi_0/2\pi)\omega$, i.e. an Ohmic resistor leads naturally to an Ohmic spectral density as mentioned before. Note that this has no cutoff, but any model of an Ohmic resistor leads to reactive behavior at high frequencies.

We see that we missed the noise term on the right, which would represent current noise originating in G and which would have to be included in a more sophisticated circuit analysis which careful engineers would do. By applying the fluctuation dissipation theorem to γ we can add on the proper noise term, whose correlation function is given by equation (15) — or we can simply use this equation with the $J(\omega)$ obtained.

We want to generalize this system now to an arbitrary shunt admittance $Y(\omega)$. For that, it comes in handy to work in Fourier space and we denote

the Fourier transform by \mathcal{F} . Analogous to eq. (27), we can find the following expression

$$-\omega^2 C \left(\frac{\Phi_0}{2\pi} \right)^2 \phi + i\omega Y(\omega) \left(\frac{\Phi_0}{2\pi} \right)^2 \phi + \mathcal{F} \left(\frac{\partial V}{\partial \phi} \right) = 0. \quad (29)$$

We have to remember that the damping Kernel γ is the Fourier cosine transform of $J(\omega)/\omega$, which also implies that it is a real valued function. We can split Y into real (dissipative) and imaginary (reactive) parts $Y = Y_d + iY_r$. For any finite electrical circuit, Y_d is always an even and Y_r always an odd function of frequency. All this allows us to rewrite eq. 29

$$-\omega^2 C \left(\frac{\Phi_0}{2\pi} \right)^2 \phi - \omega Y_r(\omega) \left(\frac{\Phi_0}{2\pi} \right)^2 \phi + i\omega Y_d(\omega) \left(\frac{\Phi_0}{2\pi} \right)^2 \phi + \mathcal{F} \left(\frac{\partial V}{\partial \phi} \right) = 0. \quad (30)$$

Thus, the general expression for the spectral density reads $J(\omega) = \omega Y_d = \omega \text{Re}Y(\omega)$, i.e. it is controlled by the *dissipative* component of $Y(\omega)$ alone. There is a new term containing the reactive component Y_r which modifies the non-dissipative part of the dynamics and can lead e.g. to mass or potential renormalization, or something more complicated. Comparing this result to the structure of the susceptibility χ in the discussion of section 1.1.2 it looks like the real and imaginary part have changed their role and there is an extra factor of ω . This is due to the fact that Y links I and V , whereas the energy-valued perturbation term in the sense of section 1.1.2 is QV . This aspects adds a time-derivative $Y = \dot{\chi}$ which leads to a factor $i\omega$ in Fourier space.

This last result can be illustrated by a few examples. If $Y(\omega) = G\Phi_0/2\pi$, we recover the previous equation (27). If the shunt is a capacitor C_s , we have $Y(\omega) = i\omega C_s$ and we get from eq. (30) the equation of motion of a particle with larger mass, parameterized by a total capacitance $C_{\text{tot}} = C_J + C_s$. On the other hand, if the shunt is an inductance L_s , we obtain $Y(\omega) = (i\omega L_s)^{-1}$, leading to a new contribution to the potential originating from the inductive energy

$$V_{\text{tot}}(\phi) = V(\phi) + \frac{(\Phi_0)^2}{8\pi^2 L} \phi^2 \quad (31)$$

and no damping term. Finally, let us consider the elementary mixed case of a shunt consisting of a resistor R_s and a capacitor C_s in series. We find $Y(\omega) = \frac{i\omega C_s}{1+i\omega R_s C_s}$ which can be broken into a damping part which is suppressed below a rolloff frequency $\omega_r = (RC)^{-1}$, $Y_d \frac{1}{R} \frac{1}{1+\omega^2/\omega_r^2}$ and a reactive part which responds capacitively below that rolloff, $Y_r = i\omega C \frac{1}{1+\omega^2/\omega_r^2}$. As the rolloffs are very soft, there is no straightforward mapping onto a

very simple model and we have to accept that the dynamics get more complicated and contain a frequency-dependent mass and friction as well as time-correlated noise, all of which gives rise to rich physics (Robertson et al., 2005).

2. Single qubit decoherence

2.1. TWO-STATE OSCILLATOR BATH MODELS

In the previous section, we introduced the notion of an oscillator bath environment for continuous systems including biased Josephson junctions. We derived quantum Langevin equation demonstrating the analogy to classical dissipative motion, but did not describe how to solve them. In fact, solving these equations in all generality is extremely hard in the quantum limit, thus a restriction of generality is sought. For our two-state systems (TSS) of interest, qubits, we are specifically interested in the case where the potential in the Hamiltonian of eq. 5 forms a double well with exactly one bound state per minimum, tunnel-coupled to each other and well separated from the higher excited levels, (Geller et al., 2006). When we also concentrate on the low-energy dynamics, we can replace the particle coordinate q by $q_0\sigma_z$ and the Hamiltonian reads

$$H = \frac{\epsilon}{2}\sigma_z + \frac{\Delta}{2}\sigma_x + \frac{\sigma_z}{2} \sum_i \lambda_i (a_i + a_i^\dagger) + \sum_i \omega_i (a_i^\dagger a_i + 1/2), \quad (32)$$

where ϵ is the energy bias and Δ is the tunnel splitting. This is the famous Spin-Boson Hamiltonian (Leggett et al., 1987; Weiss, 1999). We have dropped the counterterm, which is $\propto q^2$ in the continuous limit and, due to $q = \pm q_0$ is constant in the two-state case. The spectral density is constructed out of the $J(\omega)$ in the continuous limit

$$J_{\text{TSS}} = \sum_i \lambda_i^2 \delta(\omega - \omega_i) = \frac{q_0^2}{2\pi\hbar} J(\omega) \quad (33)$$

The Spin-Boson Hamiltonian, eq. (33) is more general than the truncation of the energy spectrum in a double-well potential may suggest. In fact, it can be derived by an alternative procedure which performs the two-state approximation first (or departs from a two-state Hamiltonian without asking for its origin) and then characterizes the bath. The oscillator bath approximation holds under the same conditions explained in section 1.1.2. The Spin-Boson model makes the assumption, that each oscillator couples to the same observable of the TSS which can always be labelled σ_z . This is

a restrictive assumption which is not necessarily true for all realizations of a dissipative two-state system.

As the two-state counterpart to classical friction used in the continuous case is not straightforward to determine, the environmental spectrum is computed from the semiclassical noise of the environment, following the prescription that, if we rewrite eq. 32 in the interaction picture with respect to the bath as

$$H_I = \frac{\epsilon + \delta\epsilon(t)}{2}\sigma_z + \frac{\Delta}{2}\sigma_x + \sum_i \omega_i (a_i^\dagger a_i + 1/2) \quad (34)$$

we can identify $\delta\epsilon$ for any physical model mapping on the Spin-Boson model as

$$\frac{1}{2} \langle \delta\epsilon(t)\delta\epsilon(0) + \delta\epsilon(0)\delta\epsilon(t) \rangle_\omega = J_{\text{TSS}}(\omega) \coth\left(\frac{\hbar\omega}{2k_B T}\right) \quad (35)$$

An application of this procedure will be presented in the next subsection.

2.1.1. Characterization of qubit environments through noise

A standard application of the characterization of the environment is the description of control electronics of relatively modest complexity, attached to a flux qubit. We look at the definite example shown in 2.1.1. It shows a simplified model of the microwave leads providing the control of a flux qubits. The microwaves inductively couple to the sample by a mutual inductance M between the qubit and a coil with self-inductance L . These leads are mounted in the cold part of the cryostat, usually on the qubit chip, and are connected to the outside world by a coaxial line which almost inevitably has an impedance of $Z = 50\Omega$. That impedance provides — in light of the discussion in the previous section — a significant source of damping and decoherence. As a design element, one can put two resistors of size R close to the coil.

The environmental noise is easily described by the Nyquist noise (Callen and Welton, 1951) of the voltage V between the arms of the circuit, see figure 2.1.1. The Johnson-Nyquist formula gives the voltage noise

$$S_V = \frac{1}{2} \langle V(t)V(0) + V(0)V(t) \rangle = \hbar\omega \text{Re}Z_{\text{eff}} \coth\left(\frac{\hbar\omega}{2k_B T}\right) \quad (36)$$

where Z_{eff} is the effective impedance between the arms, here of a parallel setup of a resistor and an inductor

$$Z_{\text{eff}} = \frac{i\omega L_{\text{eff}}R}{R + i\omega L_{\text{eff}}}, \quad (37)$$

and L_{eff} is the total impedance of the coupled set of conductors as seen from the circuit. For microwave leads, the total inductance is dominated by the self-inductance of the coil, hence $L_{\text{eff}} \approx L$.

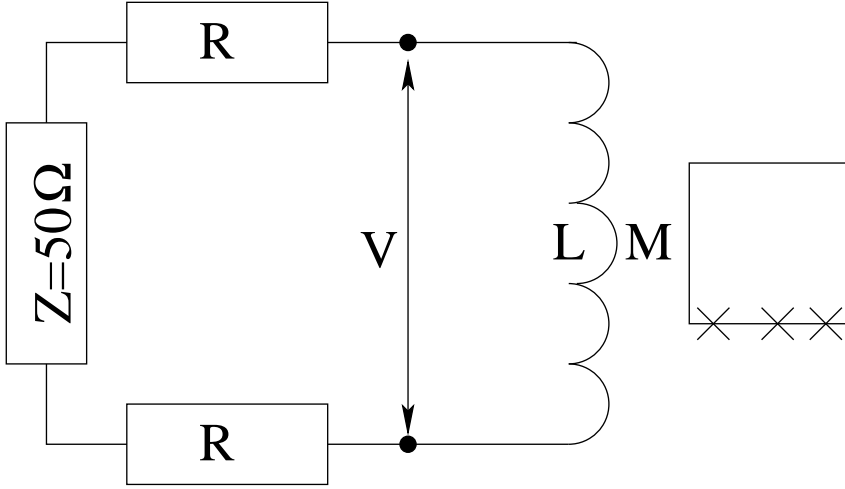


Figure 1. Typical on-chip electromagnetic environment of a superconducting flux qubit, consisting of the flux control coil with self-inductance L , mutual inductance M to the qubit, shunt impedance Z and on-chip decoupling resistors R .

We need to convert the voltage noise into energy level noise of the qubit. A voltage fluctuation δV leads to a current fluctuation in the coil following

$$\delta I = \delta V / i\omega L. \quad (38)$$

The current noise produces flux noise through the qubit loop

$$\delta\Phi = M\delta I = \frac{M}{i\omega L}\delta V \quad (39)$$

which converts into energy bias noise following

$$\delta\epsilon = I_s\delta\Phi = \frac{MI_s}{i\omega L}\delta V \quad (40)$$

with I_s being the circulating current in the potential minima of the qubit. Thus, the energy level correlation function reads

$$S_\epsilon = \left(\frac{MI_s}{i\omega L}\right)^2 S_V \quad (41)$$

which allows us to express the spectral density through the impedance as

$$J(\omega) = \hbar\omega \left(\frac{MI_s}{i\omega L}\right)^2 \text{Re}Z_{\text{eff}}(\omega). \quad (42)$$

With the specific circuit shown in figure 2.1.1, we find that the environment is Ohmic with a Drude cutoff

$$J(\omega) = \frac{\alpha\omega}{1 + \omega^2/\omega_c^2} \quad (43)$$

with $\omega_c = L/R$ and $\alpha = \frac{4M^2 I_c^2}{h(Z+2R)}$. Thus, we find a simple method to engineer the decoherence properties of the circuit with our goal being to reduce $J(\omega)$ by decoupling the device from the shunt Z . The method of choice is to put large resistors R on chip. Their size will ultimately be limited by the necessity of cooling them to cryogenic temperatures. The friction method introduced earlier, section 1.1.3, leads to the same result.

2.1.2. Linearization of nonlinear environments

In general, nonlinear environments important for qubit devices can also be identified. In superconducting devices, these include electronic environments which in addition to the linear circuit elements discussed in the previous section, also contain Josephson junctions. In general, such environments cannot be described by oscillator bath models, whose response would be strictly linear. Here, we want to concentrate on the case of a nonlinear environment — a SQUID detector — in the regime of small signal response, i.e. in a regime where it can be linearized. This linearization can be illustrated by the concept of Josephson inductance. Let us remind ourselves, that a linear inductor is defined through the following current-flux relation

$$I(\Phi) = \Phi/L \quad (44)$$

whereas the small flux-signal response of a Josephson junction can be approximated as

$$I = \sin\left(2\pi\frac{\Phi}{\Phi_0}\right) \simeq I_c \sin\left(2\pi\frac{\bar{\Phi}}{\Phi_0}\right) + \frac{\delta\Phi}{L_J} \quad (45)$$

where we have split the flux into its average $\bar{\Phi}$ and small deviations $\delta\Phi$ and have introduced the Josephson inductance $L_J = \Phi_0/2\pi I_c \cos\bar{\phi}$. Thus, the small-signal response is inductive.

We would now like to demonstrate this idea on the example of a DC-SQUID detector inductively coupled to the qubit, see fig. 2.1.2.

In the first stage, we again need to find the voltage noise between the branches of the circuit. This is given by eq. (36) with the appropriate inductance calculated from the circuit shown in the lower panel of fig. 2.1.2, $Z_{\text{eff}}^{-1} = R^{-1} + i\omega C + (i\omega L_J)^{-1}$. This is the impedance of an LC resonator with damping. The conversion into energy level noise goes along similar lines as before, incorporating the SQUID equations as described here and in standard literature (Tinkham, 1996; Clarke and Braginski, 2004).

The DC-SQUID is a parallel setup of two Josephson junctions 1 and 2, which for simplicity are assumed to be identical. The total current flowing through the device is

$$I_B = I_c(\sin\phi_1 + \sin\phi_2) = 2I_c \cos(\delta\phi/2) \sin\bar{\phi} \quad (46)$$

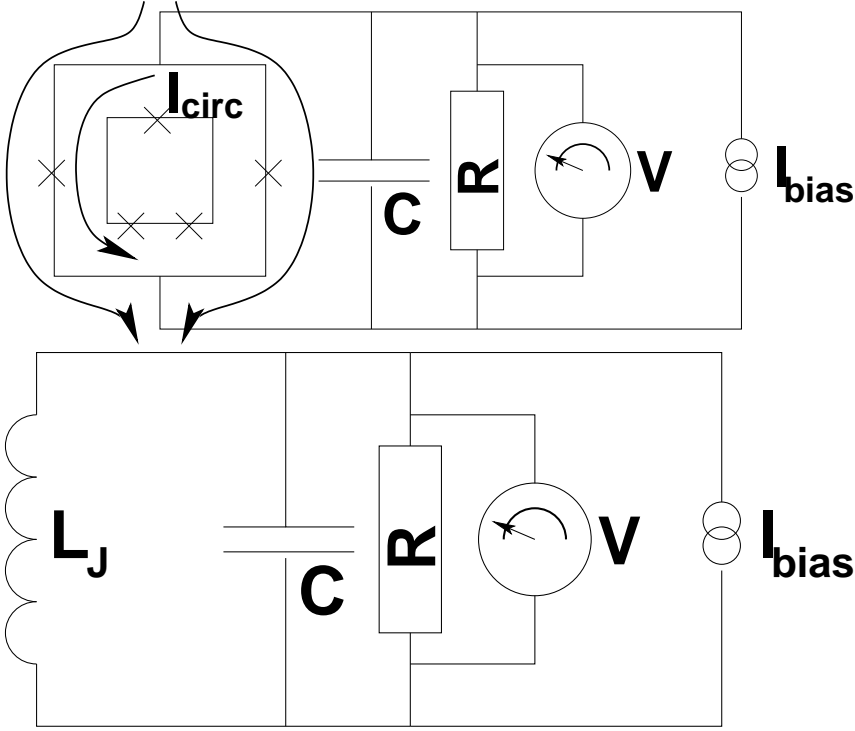


Figure 2. Upper panel: DC-SQUID readout circuit consisting of the actual SQUID, a shunt capacitor, and a voltmeter with an unavoidable resistor. Lower panel: Linearized circuit used for the noise calculation

where we have introduced $\bar{\phi} = (\phi_1 + \phi_2)/2$ and $\delta\phi = \phi_1 - \phi_2$. Now we need to remember that the phases ϕ_i are connected to the Schrödinger equation for the superconducting condensate. Thus, an elementary calculation (Tinkham, 1996; Clarke and Braginski, 2004) leads to

$$\delta\phi = 2\pi \frac{\Phi}{\Phi_0} \text{mod} 2\pi \quad (47)$$

where Φ is the total magnetic flux through the loop. This is identical to the flux applied externally using a biasing coil plus the qubit flux as we neglect self-inductance. Thus, for the bias current I_B the DC-SQUID acts like a tunable Josephson junction with a critical current $I_{c,\text{eff}}(\Phi) = 2I_c |\cos(\pi\Phi/\Phi_0)|$. Thus, we can translate voltage fluctuations into phase fluctuations as

$$\delta\bar{\phi} = \left(\frac{2\pi}{\Phi_0} \right) \frac{\delta V}{i\omega}. \quad (48)$$

The qubit is coupling to the magnetic flux which — assuming a symmetric SQUID geometry - is coupled only to the circulating current

$$I_{\text{circ}} = I_c(\sin \phi_1 - \sin \phi_2)/2 = I_c \cos(\bar{\phi}) \sin \frac{\pi \Phi}{\Phi_0}. \quad (49)$$

We can now express its fluctuations through the fluctuations of $\bar{\phi}$

$$\delta I_{\text{circ}} = -I_c \sin \frac{\pi \Phi}{\Phi_0} \sin(\bar{\phi}) \delta \bar{\phi} = \frac{I_B}{2} \tan \frac{\pi \Phi}{\Phi_0} \delta \phi \quad (50)$$

where in the last step we have used eq. 46. With the remaining steps analogous to the previous section, we obtain

$$J(\omega) = \hbar \omega \left(M I_s \frac{I_B}{2} \frac{2\pi}{\Phi_0} \tan \frac{\pi \Phi}{\Phi_0} \right)^2 \text{Re} Z_{\text{eff}}. \quad (51)$$

Here, Z_{eff} is the impedance of the linearized circuit shown in the bottom panel of fig. 2.1.2. This result reveals a few remarkable features. Most prominently, it shows that $J(\omega)$ can be tuned by shifting the working point of the linearization through changing the bias current I_B . In particular, $J(\omega)$ can be set to zero by choosing $I_B = 0$. The origin of this decoupling can be seen in eq. 50, which connects the bias current noise to the circulating current noise. The physical reason for this is, that in the absence of a bias current the setup is fully symmetric — any noise from the external circuitry splits into equal amounts on the branches of the loop and thus does not lead to flux noise. For a detector, this is a highly desired property. It allows to switch the detector off completely. When we do not bias, we have (for the traditional switching current measurement) no sensitivity and with it no backaction. This means, that if the device is really highly symmetric, one can push this device to the strong measurement regime while still being able to operate in the "off" state of the detector. This effect has been predicted in Refs. (van der Wal et al., 2003; Wilhelm et al., 2003). Experimentally, it was first observed that the decoupled point was far from zero bias due to a fabrication issue (Burkard et al., 2005), which was later solved such that our prediction has indeed been verified (Bertet et al., 2005a).

2.1.3. *The Bloch equation*

So far, we have discussed the characterization of the environment at length. We did not specify how to describe the qubit dynamics under its influence. For a continuous system, we have derived the quantum Langevin equation (11). Even though this equation looks straightforward, solving it for potentials others than the harmonic oscillator is difficult without further approximations. We will now show first how to describe decoherence in

a phenomenological way and then discuss how to reconcile microscopic modelling with the Bloch equation.

For describing the decoherence of a qubit we have to use the density matrix formalism, which can describe pure as well as mixed states. In the case of a qubit with a two-dimensional Hilbert space, we can fully parameterize the density matrix by its three spin projections $S_i = \text{Tr}(\rho\sigma_i)$, $i = x, y, z$ as

$$\rho = \frac{1}{2} \left(1 + \sum_i S_i \sigma_i \right) \quad (52)$$

where the σ_i are Pauli matrices. This notation is inspired by spin resonance and is applicable to any two-state system including those realized in superconducting qubits. We can take the analogy further and use the typical NMR notation with a strong static magnetic field $B_z(t)$ applied in one direction identified as the z -direction and a small AC field, $B_x(t)$ and $B_y(t)$ in the xy -plane. In that case, there is clearly a preferred-axis symmetry and two distinct relaxation rates, the longitudinal rate $1/T_1$ and the transversal rate $1/T_2$ can be introduced phenomenologically to yield

$$\dot{S}_z = \gamma(\vec{B} \times \vec{S})_z - \frac{S_z - S_{z,eq}}{T_1} \quad (53)$$

$$\dot{S}_{x/y} = \gamma(\vec{B} \times \vec{S})_{x/y} - \frac{S_{x/y}}{T_2} \quad (54)$$

where we have introduced the equilibrium spin projection $S_{z,eq}$ and the spin vector $\vec{S} = (S_x, S_y, S_z)^T$. Note that the coherent part of the time evolution is still present. It enters the Bloch equation via the Hamiltonian, decomposed into Pauli matrices as $H = -\gamma\vec{B} \cdot \vec{S}$. This spin notation is also useful for superconducting qubits, even though the three components usually depend very distinct observables such as charge, flux, and current. This parameterization leads to the practical visualization of the state and the Hamiltonian as a point and an axis in three-dimensional space respectively. The free evolution of the qubit then corresponds to Larmor precession around the magnetic field. The pure states of the spin have $\vec{S}^2 = 1$ and are hence on a unit sphere, the Bloch sphere, whereas the mixed states are inside the sphere — in the Bloch ball.

The rates are also readily interpreted in physical terms. As the large static field points in the z -direction in our setting, the energy dissipation is given as

$$\frac{d\langle E \rangle}{dt} = -\gamma B_z \dot{S}_z \quad (55)$$

and hence its irreversible part is given through $1/T_1$. On the other hand, the purity (or linearized entropy) $P = \text{Tr}\rho^2 = 1/4 + \sum_i S_i^2$ decays as

$$\dot{P} = 2 \sum_i \dot{S}_i S_i = -\frac{S_x^2 + S_y^2}{T_2} - \frac{S_z(S_z - S_{z,eq})}{T_1} \quad (56)$$

thus all rates contribute to decoherence. Note, that at low temperatures $S_{z,eq} \rightarrow 1$ so the T_1 -term in general augments the purity and reestablishes coherence. This can be understood as the system approaches the ground state, which is a pure state. In this light, it needs to be imposed that $P \leq 1$ as otherwise the density matrix has negative eigenvalues. This enforces $T_2 \leq 2T_1$.

2.2. SOLUTIONS OF THE BLOCH EQUATION AND SPECTROSCOPY

The rates shown in the Bloch equation are also related to typical spectroscopic parameters (Abragam, 1983; Goorden and Wilhelm, 2003). We chose a rotating driving field

$$B_x = (\omega_R/\gamma) \cos \omega t \quad (57)$$

$$B_y = (\omega_R/\gamma) \sin \omega t. \quad (58)$$

In spectroscopy, we are asking for the steady state population, i.e. for the long-time limit of S_z . Transforming the Bloch equation into the frame co-rotating with the driving field and computing the steady-state solution, we obtain

$$S_z(\omega) = \frac{\omega_R^2}{(\omega - \gamma B)^2 + \gamma^2} \quad (59)$$

with a linewidth $\gamma^2 = 1/T_2^2 + \omega_R^2 T_2/T_1$. This simple result allows spectroscopic determination of all the parameters of the Bloch equation: At weak driving, $\omega_R \sqrt{T_1 T_2} \ll 1$, the line width is $1/T_2$. This regime can be easily identified as the spectral line not being saturated, i.e. the height grows with increasing drive. In fact, the height of the resonance is $S_z(\gamma B) = \omega_R^2 T_2^2$, which (knowing $1/T_2$) allows to determine ω_R . Due to the heavy filtering between the room-temperature driving and the cryogenic environment, this is not known a priori. To determine T_1 , one goes to the high driving regime with a saturated line, i.e. a line which does not grow any more with higher power, $\omega_R \sqrt{T_1 T_2} \gg 1$ and finds a line width of $\omega_R \sqrt{T_1/T_2}$. With all other parameters known already, this allows to find T_1 . Using this approach is helpful to debug an experiment which does not work yet. Alternatively, real-time measurements of T_1 are possible under a wide range of conditions.

2.2.1. How to derive the Bloch equation: The Bloch-Redfield technique

We now show how to derive Bloch-like equations from the system-bath models we studied before using a sequence of approximations. The *Born approximation* works if the coupling between system and bath is weak. The *Markov approximation* works if the coupling between system and bath is the slowest process in the system, in particular if it happens on a time scale longer than the correlation time of the environment. Quantitatively, we can put this into the *motional narrowing condition*

$$\frac{\lambda\tau_c}{\hbar} \ll 1, \quad (60)$$

where λ is the coupling strength between the system and its environment and τ_c the correlation time of the environment. In the case treated in eq. 19 we would have $\tau_c = 1/\omega_c$. If this is satisfied, an averaging process over a time scale longer than τ_c but shorter than λ^{-1} can lead to simple evolution equations, the so-called Bloch-Redfield equations (Argyres and Kelley, 1964). The derivation in Ref. (Cohen-Tannoudji et al., 1992) follows this inspiration. We will follow the very elegant and rigorous derivation using projection operators as given in (Argyres and Kelley, 1964; Weiss, 1999). We are going to look at a quantum subsystem with an arbitrary finite dimensional Hilbert space, accomodating also qudit and multiple-qubit systems.

As a starting point for the derivation of the Bloch-Redfield equations (70), one usually (Weiss, 1999) takes the Liouville equation of motion for the density matrix of the whole system $W(t)$ (describing the time evolution of the system)

$$\dot{W}(t) = -\frac{i}{\hbar} [H_{\text{total}}, W(t)] = \mathcal{L}_{\text{total}}W(t), \quad (61)$$

where H_{total} is the total Hamiltonian and $\mathcal{L}_{\text{total}}$ the total Liouvillian of the whole system. This notation of the Liouvillian uses the concept of a *superoperator*. Superoperator space treats density matrices as vectors. Simply arrange the matrix elements in a column, and each linear operation on the density matrix can be written as a (super)matrix multiplication. Thus, the right hand side of the Liouville equation can be written as a single matrix products, not a commutator, where a matrix acts from the left and the right at the same time. Hamiltonian and Liouvillian consist of parts for the relevant subsystem, the reservoir and the interaction between these

$$H_{\text{total}} = H_{\text{sys}} + H_{\text{res}} + H_I \quad (62)$$

$$\mathcal{L}_{\text{total}} = \mathcal{L}_{\text{sys}} + \mathcal{L}_{\text{res}} + \mathcal{L}_I. \quad (63)$$

H_{sys} is the Hamiltonian which describes the quantum system (in our case: the qubit setup), H_{res} represents for the environment and H_I is the interaction Hamiltonian between system and bath.

Projecting the density matrix of the whole system $W(t)$ on the relevant part of the system (in our case the qubit), one finally gets the reduced density matrix ρ acting on the quantum system alone

$$\rho(t) = \text{Tr}_B W(t) = PW(t) , \quad (64)$$

so P projects out onto the quantum subsystem. As in the previous derivation in section 1.1.1, we need to formally solve the irrelevant part of the Liouville equation first. Applying $(1 - P)$, the projector on the irrelevant part, to eq. 61 and the obvious $W = PW + (1 - P)W$ we get

$$(1 - P)\dot{W} = (1 - P)\mathcal{L}_{\text{total}}(1 - P)W + (1 - P)\mathcal{L}_{\text{total}}\rho. \quad (65)$$

This is an inhomogenous linear equation of motion which can be solved with variation of constants, yealding

$$(1 - P)\rho(t) = \int_0^t dt' e^{(1 - P)\mathcal{L}_{\text{total}}(t - t')} (1 - P)\mathcal{L}_{\text{total}}\rho(t') + e^{(1 - P)\mathcal{L}_{\text{total}}t} (1 - P)W(0). \quad (66)$$

Putting this result into equation (61) one gets the Nakajima-Zwanzig equation (Nakajima, 1958; Zwanzig, 1960)

$$\begin{aligned} \dot{\rho}(t) = & P\mathcal{L}_{\text{total}}\rho(t) + \int_0^t dt' P\mathcal{L}_{\text{total}}e^{(1 - P)\mathcal{L}_{\text{total}}(t - t')} (1 - P)\mathcal{L}_{\text{total}}\rho(t') + \\ & + P\mathcal{L}_{\text{total}}e^{(1 - P)\mathcal{L}_{\text{total}}t} (1 - P)W(0). \end{aligned} \quad (67)$$

So far, all we did was fully exact. The dependence on the initial value of the irrelevant part of the density operator $(1 - P)W(0)$ is dropped, if the projection operator is chosen appropriately – using factorizing initial conditions, i.e. $W = \rho \otimes (1 - P)W$. A critical assesment of this assumption will be given in section 3.1.2. As P commutes with \mathcal{L}_{sys} , one finds

$$\dot{\rho} = P(\mathcal{L}_{\text{sys}} + \mathcal{L}_I)\rho(t) + \int_0^t dt' P\mathcal{L}_I e^{(1 - P)\mathcal{L}_{\text{total}}(t - t')} (1 - P)\mathcal{L}_I\rho(t'). \quad (68)$$

The reversible motion of the relevant system is described by the first (instantaneous) term of eq. (68), which contains the system Hamiltonian in \mathcal{L}_{sys} and a possible global energy shift originating from the environment

in $R\mathcal{L}_I$. The latter term can be taken into account by the redefinition $H'_S = H_S + PH_I$ and $H'_I = (1 - P)H_I$. The irreversibility is given by the second (time-retarded) term. The integral kernel in eq. (68) still consists of all powers in \mathcal{L}_I and the dynamics of the reduced density operator ρ of the relevant system depends on its own whole history. To overcome these difficulties in practically solving eq. (68), one has to make approximations. We begin by assuming that the system bath interaction is weak and restrict ourselves to the Born approximation, second order in \mathcal{L}_I . This allows us to replace \mathcal{L}_{total} by $\mathcal{L}_{sys} + \mathcal{L}_{res}$ in the exponent. The resulting equation is still nonlocal in time. As it is convolutive, it can in principle be solved without further approximations (Loss and DiVincenzo, 2003). To proceed to the more convenient Bloch-Redfield limit, we remove the memory firstly by propagating $\rho(t')$ forward to $\rho(t)$. In principle, this would require solving the whole equation first and not be helpful. In our case, however, we can observe that the other term in the integral — the kernel of the equation — is essentially a bath correlation function which only contributes at $t - t' < \tau_c$. Using the motional narrowing condition eq. 60, we see that the system is unlikely to interact with the environment in that period and we can replace the evolution of ρ with the free evolution, $\rho(t') = e^{\mathcal{L}_{sys}(t-t')}\rho(t)$. After this step, the equation is local in time, but the coefficients are still time-dependent. Now we flip the integration variable $t' \rightarrow t - t'$ and then use the motional narrowing condition again to send the upper limit of the integral to infinity, realizing that at such large time differences the kernel will hardly contribute anyway. We end up with the Bloch-Redfield equation

$$\dot{\rho}(t) = P(\mathcal{L}_{sys} + \mathcal{L}_I)\rho(t) + \int_0^\infty dt' P\mathcal{L}_I e^{(1-P)(\mathcal{L}_{sys} + \mathcal{L}_{res})t'} (1 - P)\mathcal{L}_I \rho(t). \quad (69)$$

The Bloch-Redfield equation is of Markovian form, however, by properly using the free time evolution of the system (back-propagation), they take into account all bath correlations which are relevant within the Born approximation (Hartmann et al., 2000). In (Hartmann et al., 2000), it has also been shown that in the bosonic case the Bloch-Redfield theory is numerically equivalent to the path-integral method.

The resulting Bloch-Redfield equations for the reduced density matrix ρ in the eigenstate basis of H_{sys} then read (Weiss, 1999)

$$\dot{\rho}_{nm}(t) = -i\omega_{nm}\rho_{nm}(t) - \sum_{k,\ell} R_{nmk\ell}\rho_{k\ell}(t), \quad (70)$$

where $R_{nmk\ell}$ are the elements of the Redfield tensor and the ρ_{nm} are the elements of the reduced density matrix.

The Redfield tensor has the form (Weiss, 1999; Blum, 1996)

$$R_{nmk\ell} = \delta_{\ell m} \sum_r \Gamma_{nrrk}^{(+)} + \delta_{nk} \sum_r \Gamma_{\ell rrm}^{(-)} - \Gamma_{\ell mnk}^{(+)} - \Gamma_{\ell mnk}^{(-)}. \quad (71)$$

The rates entering the Redfield tensor elements are given by the following Golden-Rule expressions (Weiss, 1999; Blum, 1996)

$$\Gamma_{\ell mnk}^{(+)} = \hbar^{-2} \int_0^{\infty} dt e^{-i\omega_{nk}t} \langle \tilde{H}_{I,\ell m}(t) \tilde{H}_{I,nk}(0) \rangle \quad (72)$$

$$\Gamma_{\ell mnk}^{(-)} = \hbar^{-2} \int_0^{\infty} dt e^{-i\omega_{\ell m}t} \langle \tilde{H}_{I,\ell m}(0) \tilde{H}_{I,nk}(t) \rangle, \quad (73)$$

where H_I appears in the interaction representation

$$\tilde{H}_I(t) = \exp(iH_{\text{res}}t/\hbar) H_I \exp(-iH_{\text{res}}t/\hbar). \quad (74)$$

ω_{nk} is defined as $\omega_{nk} = (E_n - E_k)/\hbar$. In a two-state system, the coefficients ℓ , m , n and k stand for either $+$ or $-$ representing the upper and lower eigenstates. The possible values of ω_{nk} in a TSS are $\omega_{++} = \omega_{--} = 0$, $\omega_{+-} = \frac{2\delta}{\hbar}$ and $\omega_{-+} = -\frac{E}{\hbar}$, where E is the energy splitting between the two charge eigenstates with $E = \sqrt{\epsilon^2 + \Delta^2}$. Now we apply the secular approximation, which again refers to weak damping, to discard many rates in the Redfield tensor as irrelevant. The details of this approximation are most transparent in the multi-level case and will be discussed in more detail in section 4.0.4. In the TSS case, the secular approximation holds whenever the Born approximation holds. After the secular approximation, the Bloch-Redfield equation coincides with the Bloch equation with

$$1/T_1 = \sum_n R_{nnnn} = R_{++++} + R_{----} = \Gamma_{-+-} + \Gamma_{-+-} \quad (75)$$

$$\begin{aligned} 1/T_2 &= \text{Re}(R_{nmnm}) = \text{Re}(R_{+--+}) = \text{Re}(R_{-+-}) \\ &= \text{Re}(\Gamma_{+--+} + \Gamma_{-+-} + \Gamma_{----} + \Gamma_{++++} - \Gamma_{-+-} - \Gamma_{+--+}). \\ &= \frac{1}{2T_1} + \frac{1}{T_\phi} \end{aligned} \quad (76)$$

Here, we have introduced the dephasing rate T_ϕ^{-1} . The relaxation rate is given by the time evolution of the *diagonal* elements, and the dephasing rate by the *off-diagonal* elements of the reduced density matrix ρ .

The factor of two in the formula connecting $1/T_2$ and $1/T_1$ appears to be counterintuitive, as we would expect that energy relaxation definitely also leads to dephasing, without additional factors. This physical picture is

also correct, but one has to take into account that there are *two* channels for dephasing — clockwise and counterclockwise precession — which need to be added. In fact, this is the reason why the same factor of two appears in the positivity condition for the density matrix, see section 2.1.3. Another view is to interpret the diagonal matrix elements as classical probabilities, the absolute square of a eigenfunctions of the Hamiltonian, $|\psi_1|^2$, whereas the off-diagonal terms constitute amplitudes, $\psi_2^*\psi_1$. Being squares, probabilities decay twice as fast as amplitudes. This point will be discussed further later on in the context of multi-level decoherence, eq. 106.

The imaginary part of the Redfield tensor elements that are relevant for the dephasing rate $\Im(R_{+-+})$ provides a renormalization of the coherent oscillation frequency ω_{+-} , $\delta\omega_{+-} = \Im(\Gamma_{+--+} + \Gamma_{-++-})$. If the renormalization of the oscillation frequency gets larger than the oscillation frequency itself, the Bloch-Redfield approach with its weak-coupling approximations does not work anymore. By this, we have a direct criterion for the validity of the calculation.

Finally, the stationary population is given by

$$S_{z,eq} = \frac{\Gamma_{-+++} - \Gamma_{+--+}}{\Gamma_{-+++} + \Gamma_{+--+}} = \tanh\left(\frac{\hbar\omega_{+-}}{2k_B T}\right) \quad (77)$$

where in the last step we have used the property of detailed balance

$$\Gamma_{nmnm} = \Gamma_{mnmn} e^{-\omega_{mn}/k_B T} \quad (78)$$

which holds for any heat bath in thermal equilibrium and is derived e.g. in References (Weiss, 1999; Ingold, 1998; Callen and Welton, 1951).

A different kind of derivation with the help of Keldysh diagrams for the specific case of an single-electron transistor (SET) can be found in the Appendix of Ref. (Makhlin et al., 2001).

Very recent results (Gutmann and Wilhelm, 2006; Thorwart et al., 2005) confirm that without the secular approximation, Bloch-Redfield theory preserves complete positivity only in the pure dephasing case (with vanishing coupling $\Delta = 0$ between the qubit states). In all other cases, complete positivity is violated at short time scales. Thus only in the pure dephasing regime is the Markovian master equation of Lindblad form (Lindblad, 1976) as typically postulated in mathematical physics. In all other cases the Lindblad theorem does *not* apply. This is not an argument against Bloch-Redfield — the Markovian shape has been obtained as an approximation which coarse-grains time, i.e. it is not supposed to be valid on short time intervals. Rather one has to question the generality of the Markov approximation (Lidar et al., 2004) at low temperature. Note, that in some cases the violation of positivity persists and one has to resort to more elaborate tools for consistent results (Thorwart et al., 2005)

2.2.2. Rates for the Spin-Boson model and their physical meaning

This technique is readily applied to the spin boson Hamiltonian eq. (32). The structure of the golden rule rates eqs. (72 and 73) become rather transparent — the matrix elements of the interaction taken in the energy eigenbasis measure symmetries and selection rules whereas the time integral essentially leads to energy conservation.

In particular, we can identify the energy relaxation rate

$$\frac{1}{T_1} = \frac{\Delta^2}{E^2} S(E). \quad (79)$$

The interpretation of this rate is straightforward — the system has to make a transition, exchanging energy E with the environment using a single Boson. The factor $S(E) = J(E)(n(E) + 1 + n(E))$ captures the density of Boson states $J(E)$ and the sum of the rates for emission proportional to $n(E) + 1$ and absorption proportional to $n(E)$ of a Boson. Here, $n(E)$ is the Bose function. The prefactor is the squared cosine of the angle between the coupling to the noise and the qubit Hamiltonian, i.e. it is maximum if — in the basis of qubit eigenstates — the bath couples to the qubit in a fully off-diagonal way. This is reminiscent of the standard square of the transition matrix element in Fermi's golden rule.

The flip-less contribution to T_2 reads

$$\frac{1}{T_\phi} = \frac{\epsilon^2}{2E^2} S(0). \quad (80)$$

It accounts for the dephasing processes which do not involve a transition of the qubit. Hence, they exchange zero energy with the environment and $S(0)$ enters. The prefactor measures which fraction of the total environmental noise leads to fluctuations of the energy splitting, i.e., it is complementary to the transition matrix element in T_1 — the component of the noise *diagonal* in the basis of energy eigenstates leads to pure dephasing. The zero frequency argument is a consequence of the Markov approximation. More physically, it can be understood as a limiting procedure involving the duration of the experiment, which converges to $S(0)$ under the motional narrowing condition. Details of this procedure and its limitations will be discussed in the next section.

Finally, the energy shift

$$\delta E = \frac{\Delta^2}{E^2} \mathcal{P} \int d\omega \frac{J(\omega)}{E^2 - \omega^2}, \quad (81)$$

where \mathcal{P} denotes the Cauchy mean value, is analogous to the energy shift in second order perturbation theory, which collects all processes in which a

virtual Boson is emitted and reabsorbed, i.e. no trace is left in the environment. Again, the prefactor ensures that the qubit makes a virtual transition during these processes. For the Ohmic case, we find

$$\delta E = \alpha E \frac{\Delta^2}{E^2} \log\left(\frac{\omega_c}{E}\right) \quad (82)$$

provided that $\omega_c \gg E$. Thus, the energy shift explicitly depends on the ultraviolet cutoff. In fact, $\delta E \simeq E$ would be an indicator for the breakdown of the Born approximation. Thus, we can identify two criteria for the validity of this approximation, $\alpha \ll 1$ and $\alpha \log(\omega_c/E) \ll 1$. The latter is more confining, i.e. even if the first one is satisfied, the latter one can be violated. Note that in some parts of the open quantum systems literature, the justification and introduction of this ultraviolet cutoff is discussed extensively. The spectral densities we have computed so far in the previous sections have always had an intrinsic ultraviolet cutoff, e.g. the pure reactive response of electromagnetic circuits at high frequencies.

2.3. ENGINEERING DECOHERENCE

The picture of decoherence we have at the moment apparently allows to engineer the decoherence properties — which we initially perceived as something deep and fundamental — using a limited set of formulae, eqs. 79, 80 and 42, see Refs. (van der Wal et al., 2003; Makhlin et al., 2001) these equations have been applied to designing the circuitry around quantum bits. This is, however, not the end of the story. After this process had been mastered to sufficient degree, decoherence turned out to be limited by more intrinsic phenomena, and by phenomena not satisfactorily described by the Bloch-Redfield technique. This will be the topic of the next section.

3. Beyond Bloch-Redfield

It is quite surprising that a theory such as Bloch-Redfield, which contains a Markov approximation, works so well at the low temperatures at which superconducting qubits are operated, even though correlation functions at low temperatures decay very slowly and can have significant power-law time tails. The main reason for this is the motional narrowing condition mentioned above, which essentially states that a very severe Born approximation, making the system-bath interaction the lowest energy/longest time in the system, will also satisfy that condition. This is analogous to the textbook derivation of Fermi's golden rule (Cohen-Tannoudji et al., 1992; Sakurai, 1967), where the perturbative interaction is supposed to be

the slowest process involved. In this section, we are going to outline the limitations of this approach by comparing to practical alternatives.

Before proceeding we would also like to briefly comment on the general problem of characterizing the environment in an open quantum system. The most general environment is usually assumed to induce a completely positive linear map (or "quantum operation") on the reduced density matrix. The most general form of such a map is known as the Krauss operator-sum representation, although such a representation is not unique, even for a given microscopic system-bath model like the one considered here. A continuous-time master equation equivalent to a given Krauss map is provided by the Lindblad equation, but the form of the Lindblad equation is again not unique. The Lindblad equation gives the most general form of an equation of motion for the reduced density matrix that assures complete positivity and conserves the trace; however, the Markov and Born approximations are often needed to construct the specific Lindblad equation corresponding to a given microscopic model. The Markov approximation is a further additional simplification, rendering the dynamics to that of a semigroup. A semigroup lacks an inverse, in accordance with the underlying time-irreversibility of an open system. However, like the unitary group dynamics of a closed system, the semigroup elements can be generated by exponentials of non-Hermitian "Hamiltonians", greatly simplifying the analysis. The Bloch-Redfield master equation also has a form similar to that of the Lindblad equation, but there is one important difference: Bloch-Redfield equation does not satisfy complete positivity for all values of the diagonal and off-diagonal relaxation parameters. If these parameters are calculated microscopically (or are obtained empirically), then complete positivity will automatically be satisfied, and the Bloch-Redfield equation will be equivalent to the Lindblad equation. Otherwise inequalities have to be satisfied by the parameters in order to guarantee complete positivity.

3.1. PURE DEPHASING AND THE INDEPENDENT BOSON MODEL

We start from the special case $\Delta = 0$ of the spin-Boson model, also known as the independent Boson model (Mahan, 2000). We will discuss, how this special case can be solved exactly for a variety of initial conditions. Restricting the analysis to this case is a loss of generality. In particular, as the qubit part of the Hamiltonian commutes with the system-bath coupling, it cannot induce transitions between the qubit eigenstates. Thus $1/T_1 = 0$ to all orders as confirmed by eq. 79 and $1/T_2 = S(0)$ following eq. 80. Still, it allows to gain insight into a number of phenomena and the validity of the standard approximations. Moreover, the results of this section have been

confirmed based on a perturbative diagonalization scheme valid for gap or super-ohmic environmental spectra (Wilhelm, 2003).

3.1.1. Exact propagator

As the qubit and the qubit-bath coupling commute, we can construct the exact propagator of the system. We go into the interaction picture. The system-bath coupling Hamiltonian then reads

$$H_{SB}(t) = \frac{1}{2}\sigma_z \sum_j \lambda_j (a_j e^{-i\omega_j t} + a_j^\dagger e^{i\omega_j t}). \quad (83)$$

The commutator of this Hamiltonian with itself taken at a different time is a c-number. Consequently, up to an irrelevant global phase, we can drop the time-ordering operator \mathcal{T} in the propagator (Sakurai, 1967; Mahan, 2000) and find

$$\begin{aligned} U(t, t') &= \mathcal{T} \exp\left(-\frac{i}{\hbar} \int_{t'}^t dt' H_{SB}(t')\right) \\ &= \exp\left(\sigma_z \sum_i \frac{\lambda_i}{2\hbar\omega_i} \left(a_i^\dagger \left(e^{i\omega_i(t-t')-1}\right) - a_i \left(e^{-i\omega_i(t-t')-1}\right)\right)\right). \end{aligned} \quad (84)$$

In order to work with this propagator, it is helpful to reexpress it using shift operators $D_i(\alpha_i) = \exp(\alpha a_i^\dagger - \alpha^* a_i)$ as

$$U(t, t') = \prod_j D_j \left(\sigma_z \frac{\lambda_j}{2\hbar\omega_j} \left(e^{i\omega_j(t-t')} - 1 \right) \right). \quad (85)$$

This propagator can be readily used to compute observables. The main technical step remains to trace over the bath using an appropriate initial state. The standard choice, also used for the derivation of the Bloch-Redfield equation, is the factorized initial condition with the bath in thermal equilibrium, i.e. the initial density matrix

$$\rho(0) = \rho_q \otimes e^{-H_B/kT} \quad (86)$$

where we use the partition function Z (Landau and Lifshitz, 1984). The expectation value of the displacement operator between number states is $\langle n | D(\alpha) | n \rangle = e^{-(2n+1)|\alpha|^2/2}$. We start in an arbitrary pure initial state of the qubit

$$\rho_q = |\psi\rangle \langle \psi|, \quad |\psi\rangle = \cos \frac{\theta}{2} |0\rangle + \sin \frac{\theta}{2} e^{i\phi} |1\rangle. \quad (87)$$

Using these two expressions, we can compute the exact reduced density matrix, expressed through the three spin projections

$$\langle \sigma_x \rangle(t) = \sin \theta \cos(Et + \phi) e^{-K_f(t)} \quad (88)$$

$$\langle \sigma_y \rangle (t) = \sin \theta \sin(Et + \phi) e^{-K_f(t)} \quad (89)$$

$$\langle \sigma_z \rangle (t) = \cos \theta \quad (90)$$

where we have introduced the exponent of the envelope for factorized initial conditions,

$$K_f(t) = \int \frac{d\omega}{\omega^2} S(\omega) (1 - \cos \omega t) \quad (91)$$

which coincides with the second temporal integral of the semiclassical correlation function $S(t)$, see eq. 18. What does this expression show to us? At short times, we always have $K_f(t) \propto \frac{t^2}{2} \int d\omega S(\omega)$, which is an integral dominated by large frequencies and thus usually depends on the cutoff of $S(\omega)$. At long times, it is instructive to rewrite this as

$$K_f(t) = t \int d\omega \delta_\omega(t) S(\omega) \quad (92)$$

where we have introduced $\delta_\omega(t) = 2 \frac{\sin^2 \omega t / 2}{\omega^2 t}$, which approaches $\delta(\omega)$ as $t \rightarrow \infty$. Performing this limit more carefully, we can do an asymptotic long-time expansion. Long refers to the internal time scales of the noise, i.e. the reciprocal of the internal frequency scales of $S(\omega)$, including \hbar/kT , ω_c^{-1} . The expansion reads

$$K_f(t) = -t/T_2 + \log v_F + O(1/t) \quad (93)$$

with $1/T_2 = S(0)$ as in the Bloch-Redfield result and $\log v_F = \mathcal{P} \int \frac{d\omega}{\omega^2} S(\omega)$. Here, \mathcal{P} is the Cauchy mean value regularizing the singularity at $\omega = 0$. To highlight the meaning of v_F , the visibility for factorized initial conditions, we plug this expansion into eq. 88 and see that $\langle \sigma_x \rangle (t) = v_F \sin \theta \cos(Et + \phi) e^{-t/T_2 + O(1/t)}$. Thus, a long-time observer of the full dynamics sees exponential decay on a time scale T_2 which coincides with the Bloch-Redfield result for the pure dephasing situation, but with an overall reduction of amplitude by a factor $v < 1$. This is an intrinsic loss of visibility (Vion et al., 2002; Simmonds et al., 2004). Several experiments have reported a loss of visibility, to which this may be a contribution. Note that by improving detection schemes, several other sources of reduced visibility have been eliminated (Lupascu et al., 2004; Wallraff et al., 2005).

This result allows a critical assessment of the Born-Markov approximation we used in the derivation of the Bloch-Redfield equation. It fails to predict the short-time dynamics — which was to be expected as the Markov approximation is essentially a long-time limit. In the long time limit, the exponential shape of the decay envelope and its time constant are predicted correctly, there are no higher-order corrections to T_2 at the pure dephasing point. The value of T_2 changes at finite Δ , see Refs. (Leggett

et al., 1987; Weiss, 1999; Wilhelm, 2003). A further description of those results would however be far beyond the scope of this chapter and can be found in ref (Wilhelm, 2003). Finally, we can see how both short and long-time dynamics are related: the short-time (non-Markovian) dynamics leaves a trace in the long-time limit, namely a drop of visibility.

We now give examples for this result. In the Ohmic case $J(\omega) = \alpha\omega e^{-\omega/\omega_c}$ at $T = 0$. Hence, we can right away compute $\dot{K}_f(t)$ and obtain $K_f(t) = \frac{\alpha}{2} \log(1 + (\omega_c t)^2)$ by a single time integral. In agreement with the formula for T_2 , see eqs. 76, 80, the resulting decay does not have an exponential component at long time but keeps decaying as a power law, indicating vanishing visibility.

At finite temperature, the computation follows the same idea but leads to a more complicated result. We give the expression from Ref. (Görlich and Weiss, 1988) for a general power-law bath $J_q(\omega) = \alpha_q \omega^q \omega_c^{1-q} e^{-\omega/\omega_c}$,

$$K_f(t) = 2\text{Re} \left\{ \alpha_q \Gamma(q-1) \left(1 - (1 + i\omega_c t)^{1-s} + \left(\frac{\hbar\omega_c}{kT} \right) \times \right. \right. \quad (94)$$

$$\left. \left. \times \left[2\zeta(s-1, \Omega) - \zeta\left(s-1, \Omega + \frac{ikTt}{\hbar}\right) - \zeta\left(q-1, \Omega - \frac{ik\tau kT}{\hbar}\right) \right] \right) \right\}$$

where we have introduced $\Omega = 1 + k_B T / \hbar \omega_0$ and the generalized Riemann zeta function, see (Abramowitz and Stegun, 1965) for the definition and the mathematical properties used in this subsection. This exact result allows to analyze and quantify the decay envelope by computing the main parameters of the decay, v_F and $1/T_2$. We will restrict ourselves to the scaling limit, $\omega_c \gg 1/t, kT$. For the Ohmic case, $q = 1$, we obtain at finite temperature $1/T_2 = 2\alpha kT/\hbar$ and $v_F = (kT/\omega_c)^\alpha$. This result is readily understood. The form of T_2 accounts for the fact that an Ohmic model has low-frequency noise which is purely thermal in nature. The visibility drops with growing ω_c indicating that if we keep adding high frequency modes they all contribute to lost visibility. It is less intuitive that v_F drops with lowering the temperature, as lowering the temperature generally reduces the noise. This has to be discussed together with the $1/T_2$ -term, remembering that $1/T_2$ is the leading and v_F only the sub-leading order of the long time expanding eq. 93: At very low temperatures, the crossover to the exponential long-time decay starts later and the contribution of non-exponential short time dynamics gains in relative significance. Indeed, at any given time, the total amplitude gets enhanced by lowering the temperature.

In order to emphasize these general observations, let us investigate the super-Ohmic case with $q \geq 3$. Such spectral functions can be realized in electronic circuits by RC-series shunts (Robertson et al., 2005), they also play a significant role in describing phonons. For $q > 3$, the exponential

component vanishes, $1/T_2 = 0$ and $v_q = \exp[-2\alpha_q\Gamma(q-1)]$. Thus, we obtain a massive loss of visibility but no exponential envelope at all. This highlights the fact that v and $1/T_2$ are to be considered independent quantifiers of non-Markovian decoherence and that the latter accounts for environmental modes of relatively low frequency whereas v is mostly influenced by the fast modes between the qubit frequency and the cutoff.

Before outlining an actual microscopic scenario, we generalize the initial conditions of our calculation.

3.1.2. *Decoherence for non-factorizing initial conditions*

Our propagator, eq. 85, is exact and can be applied to any initial density matrix. We start from an initial wave function

$$|\psi\rangle = |0\rangle \prod_n D(z_i^0/2\lambda_i\hbar\omega_i) |0\rangle_i + |1\rangle \prod_n D(z_i^1/2\lambda_i\hbar\omega_i) |0\rangle_i \quad (95)$$

where we have introduced sets of dimensionless coefficients $z_i^{0/1}$. It would be straightforward to introduce θ and ϕ , which we will stay away from in order to keep the notation transparent. The factorized initial condition corresponds to $z_i^{0/1} = 0$.

This structure has been chosen in order to be able to obtain analytical results, using the structure of the propagator expressed in displacement operators, eq. 85 and the multiplication rules for these operators (Walls and Milburn, 1994). Note that the choice of coherent states to entangle the qubit with is not a severe restriction. It has been shown in quantum optics in phase space, that essentially each density matrix of an harmonic oscillator can be decomposed into coherent states using the Wigner or Glauber P phase space representations, see e.g. (Schleich, 2001). Physically, the initial state eq. 95 corresponds to the qubit being in a superposition of two dressed states. Of specific significance is the initial condition which minimizes the system bath-interaction in the Hamiltonian eq. 32, namely $z_i^0 = -z_i^{-1} = -1$.

We can again compute all three spin projections of the qubit. The essence of the decoherence behavior is captured in the symmetric initial state, $z_i^0 = -z_i^1$ for all i

$$\langle\sigma\rangle_x = \cos Ete^{-K(t)} \quad (96)$$

very similar to eq. 88 in the factorized case, but now with

$$K(t) = -\frac{1}{2} \int_0^\infty \frac{d\omega}{\omega^2} J(\omega) \left[(u(\omega) + 1)^2 + v^2(\omega) + 1 - 2(1 + u(\omega) \cos \omega t + v(\omega) \sin \omega t) \right]$$

where we have taken a continuum limit replacing the complex numbers z_i^0 by the real function $u(\omega) + iv(\omega)$. This form connects to the factorized case by setting $u = v = 0$. For any other choice of u and v , the initial conditions are entangled.

We can make a few basic observations using this formula: The initial amplitude $e^{-K(0)}$ is controlled through

$$K(0) = \int \frac{d\omega}{2\omega^2} [u^2(\omega) + v^2(\omega)], \quad (97)$$

thus for any initial condition which is more than marginally entangled (meaning that the integral is nonzero), the initial amplitude is smaller than unity. On the other hand, the time-dependence of $K(t)$ can be completely eliminated by choosing an initial condition $u = -1, v = 0$. This condition minimizes the system-bath part of the total energy in the sense of variation with respect to u and v . This choice of initial state also minimizes the total energy if the oscillators are predominantly at high frequency, whereas for the global minimum one would rather choose a factorized state for the low-frequency oscillators. Physically, this corresponds to an optimally dressed state of the qubit surrounded by an oscillator dressing cloud. The overlap of these clouds reduces the amplitude from the very beginning but stays constant, such that the long-time visibility

$$v_g = \int \frac{d\omega}{2\omega^2} [(u(\omega) - 1)^2 + 1 + v^2(\omega)], \quad (98)$$

is maximum. Note that this reduces to the result for v_F for $u = v = 0$.

What can we learn from these results? We appreciate that initial conditions have a significant and observable effect on the decoherence of a single qubit. The choice of the physically appropriate initial condition is rather subtle and depends on the experiment and environment under consideration. A free induction decay experiment as described here does usually not start out of the blue. It is launched using a sequence of preparation pulses taking the state from a low temperature thermal equilibrium to the desired initial polarization of the qubit. Thus, from an initial equilibrium state (for some convenient setting of the qubit Hamiltonian), the fast preparation sequence initiates nonequilibrium correlations thus shaping u and v . Furthermore, if the interaction to the environment is tunable such as in the case of the detectors discussed previously in section 2.1.2, the initial condition interpolates between factorized (rapid switching of the qubit-detector coupling) and equilibrium (adiabatic switching).

At this point, we can draw conclusions about the microscopic mechanism of the loss of visibility and other short-time decoherence dynamics. The picture is rooted on the observation that the ground state of the coupled

system is a dressed state. On the one hand, as described above, the overlap of the dressing clouds reduces the final visibility. On the other hand, for nonequilibrium initial conditions such as the factorized one, there is extra energy stored in the system compared to the dressed ground state. This energy gets redistributed while the dressing cloud is forming, making it possible for an excitation in the environment with an extra energy δE to be created leading to a virtual intermediate state, followed by another excitation relaxing, thus releasing the energy δE again. It is crucial that this is *another* excitation as only processes which leave a trace in the environment lead to qubit dephasing. Higher-order processes creating and relaxing the *same* virtual excitation only lead to renormalization effects such as the Lamb shift, see eq. 81. This explains why the loss of visibility is minimal for dressed initial conditions, where no surplus excitations are present.

The Bloch-Redfield technique is a simple and versatile tool which makes good predictions of decoherence rates at low damping. At higher damping, these rates are mostly joined by renormalization effects extending the Lamb shift in eq. 81, see Refs. (Leggett et al., 1987; Weiss, 1999; Wilhelm, 2003). However, there is more to decoherence than a rate for accurate predictions of coherence amplitudes as a function of time, one has to take the non-exponential effects into account and go beyond Bloch-Redfield. Other approaches can be applied to this system such as rigorous (Born but not Markov) perturbation theory (Loss and DiVincenzo, 2003), path-integral techniques (Leggett et al., 1987), (Weiss, 1999), and renormalization schemes (Kehrein and Mielke, 1998).

Note, that these conclusions all address free induction decay. There is little indication on the quality of the Bloch-Redfield theory in the presence of pulsed driving.

3.1.3. $1/f$ noise

In the previous sections we have explored options how to engineer decoherence by influencing the spectral function $J(\omega)$ e.g. working with the electromagnetic environment. This has helped to optimize superconducting qubit setups to a great deal, down to the level where the noise intrinsic to the material plays a role. In superconductors, electronic excitations are gapped (Tinkham, 1996) and the electron phonon interaction is weak due to the inversion symmetry of the underlying crystal everywhere except close to the junctions (Ioffe et al., 2004). The most prominent source of intrinsic decoherence is thus $1/f$ noise. $1/f$ noise - noise whose spectral function behaves following $S(\omega) \propto 1/\omega$, is ubiquitous in solid-state systems. This spectrum is very special as all the integrals in our discussion up to now would diverge for that spectrum. $1/f$ typically occurs due to slowly moving defects in strongly disordered materials. In Josephson devices, there

is strong evidence for $1/f$ noise of gate charge, magnetic flux, and critical current, leading to a variety of noise coupling operators (see Ref. (Harlingen et al., 1988) for an overview). Even though there does not appear to be a fully universal origin, a "standard" model of $1/f$ noise has been identified (Dutta and Horn, 1981; Weissman, 1988): The fundamental unit are two-state fluctuators, i.e. two state systems which couple to the device under consideration and which couple to an external heat bath making them jump between two positions. The switching process consists of uncorrelated switching events, i.e. the distribution of times between these switches is Poissonian. If we label the mean time between switches as τ , the spectral function of this process is $S_{RTN} = S_0 \frac{1/\tau}{1+\tau^2\omega^2}$. This phenomenon alone is called random telegraph noise (RTN). Superimposing such fluctuators with a flat distribution of switching times leads to a total noise spectrum proportional to $1/f$. Nevertheless, the model stays different from an oscillator bath. The underlying thermodynamic limit is usually not reached as it is approached more slowly: Even a few fluctuators resemble $1/f$ noise within the accuracy of a direct noise measurement. Moreover, as we are interested in very small devices such as qubits, only a few fluctuators are effective and experiments can often resolve them directly (Wakai and van Harlingen, 1987). Another way to see this is to realize that the RTN spectrum is highly non-Gaussian: A two - state distribution can simply not be fitted by a single Gaussian, all its higher cumulants of distribution are relevant. This non-Gaussian component only vanishes slowly when we increase the system size and is significant for the case of qubits.

A number of studies of models taking this aspect into account have been published (Paladino et al., 2002; Grishin et al., 2005; Shnirman et al., 2005; Galperin et al., 2003; Faoro et al., 2005; de Sousa et al., 2005). A highly simplified version is to still take the Gaussian assumption but realize that there is always a slowest fluctuator, thus the integrals in $K_f(t)$ can be cut off at some frequency ω_{IR} at the infrared (low frequency) end of the spectrum, i.e. using the spectral function

$$S(\omega) = \frac{E_{1/f}^2}{\omega} \theta(\omega - \omega_{IR}) \quad (99)$$

with θ the Heaviside unit step function, we approximately find (Cottet, 2002; Martinis et al., 2003; Shnirman et al., 2002)

$$e^{-K(t)} \simeq (\omega_{IR} t)^{-(E_{1/f} t / \pi \hbar^2)^2} \quad (100)$$

so we find the Gaussian decay typical for short times - short on the scale of the correlation time of the environment, which is long as the spectrum is dominated by low frequencies - with a logarithmic correction.

At the moment, forefront research works at understanding more detailed models of $1/f$ noise and understand the connection between the strong dephasing and a possible related relaxation mechanism at high frequencies. On the other hand, experiments work with materials to avoid $1/f$ -noise at its source. Generally, slow noise up to a certain level can be tolerated using refocusing techniques such as simple echo or the Carr-Purcell-Gill-Meiboom pulse sequence (Gutmann et al., 2005; Carr and Purcell, 1954; Faoro and Viola, 2004; Falci et al., 2004; Shiokawa and Lidar, 2004; Bertet et al., 2005b), the power and potential of which has been demonstrated both experimentally and theoretically.

4. Decoherence in coupled qubits

To conclude, we want to outline how to go beyond a single to multiple qubits and identify the underlying challenges. On that level, much less is known both theoretically and experimentally. The variety of physically relevant Hamiltonians is larger. One extreme case is fully uncorrelated noise, e.g. originating from effects in the junctions or qubit-specific Hamiltonians,

$$H = H_{Q1} + H_{Q2} + H_{QQ} + H_{Q1B1} + H_{B1} + H_{Q2B2} + H_{B2} \quad (101)$$

this is simply the sum of two single-qubit decoherence Hamiltonians in distinct Hilbert spaces, consisting of qubit Hamiltonians H_{Qi} , $i = 1, 2$, baths H_{Bi} , qubit-bath interaction H_{QiBi} all interacting via a qubit-qubit interaction H_{QQ} alone. The other extreme case is collective noise, e.g. long-wavelength ambient fluctuations or noise shared control lines. This is described by

$$H = H_{Q1} + H_{Q2} + H_{QQ} + H_{Q1B} + H_{Q2B} + H_B \quad (102)$$

where both qubits talk to a single bath. The distinction of baths may seem artificial, as this is a special case of Hamiltonian 101: What we really mean is that in the interaction picture there is a significant correlation between baths $\langle H_{Q1B}(t)H_{Q2B}(t') \rangle \neq 0$. Note, that intermediate cases between these, a partially correlated model (Storz et al., 2005a), can be identified in the context of quantum dots.

4.0.4. The secular approximation

What does it take to study decoherence here or in other multilevel systems? Basically we can follow all the steps through the derivation of the Bloch-Redfield equation given in section 2.2.1 up to eq. 74 until we solve the equation. There, we have already mentioned the secular approximation without explaining its details.

The essence of the secular approximation is the separation of time scales. We go back to the interaction representation of equation 70, leading to

$$\dot{\rho}_{nm}^I = \sum_{kl} R_{nmkl} e^{i(\omega_{nm} - \omega_{kl})t} \rho_{kl}^I. \quad (103)$$

As the Bloch-Redfield equation is based on a Born approximation, we can expect $|R_{ijkl}| \ll \omega_{mn}$ for all coefficients i, j, k, l, m, n with $m \neq n$.

In the *secular limit*, this also holds true for most frequency splittings

$$|\omega_{nm} - \omega_{kl}| \gg |R_{nmkl}| \quad (104)$$

besides the inevitable exceptions of $n = m$, $k = l$, and $n = k$ and $m = l$. Whenever condition eq. 104 is satisfied, the time evolution induced by R_{nmkl} is certainly slower than the precession with $\omega_{nm} - \omega_{kl}$ and averages out quickly, hence it can be dropped. So the only remaining rates are the cases just mentioned:

For $n = k, m = l$, we have to keep R_{nmnm} . This rate is the dephasing rate for the transition between levels nm , see eq. 80. These rates depend on the pair of levels we chose and in general they will all be different for different choices of n and m , leading to $N(N-1)/2$ different T_2 -rates for an N -level system.

For $n = m$ and $k = l$. The set of these terms splits off from the rest of the equation, i.e. the diagonal terms of the density matrix (in the eigenstate basis) decay independent from the off-diagonal terms and obey the following set of equations

$$\dot{P}_n = \sum_n (P_m \Gamma_{m \rightarrow n} - P_n \Gamma_{n \rightarrow m}) \quad (105)$$

which is analogous to the Pauli master equation for classical probabilities. We have identified $P_n = \rho_{nn}$, the classical probability and the transition rates $\Gamma_{n \rightarrow m} = R_{nnmm}$. Equation 79 can be solved by Laplace transform, where it reduced to a matrix inversion. This leads to N different independent energy relaxation channels whose rates are the eigenvalues of the matrix form of the right hand side of eq. 105. One of these eigenvalues is always zero representing stable thermodynamic equilibrium which does not decay. In the two-state case, this leads us to one nonvanishing T_1 rate representing the only nonzero eigenvalue, given by eq. 79. The rates generally obey the positivity constraint

$$\sum_n R_{nnnn} \leq 2 \sum_{n \neq m} R_{nmnm} \quad (106)$$

the left hand side being the trace of the relaxation matrix, i.e. the sum over all T_1 -type rates and the right hand side being the sum over dephasing rates. This reduces to $T_2 \leq 2T_1$ in a two-state system.

In the opposite case, the case of an approximate *Liouvillian degeneracy*, we find a pair of frequencies $|\omega_{nm} - \omega_{kl}| \ll |R_{nmkl}|$ which do not obey the conditions mentioned in the previous paragraph, such that the secular approximation does not apply to this set of levels and R_{ijkl} must be kept. In that case, the Bloch-Redfield equation can still be diagonalized numerically, identifying the relevant modes of decay (van Kampen, 1997). Note, that Liouvillian degeneracies can appear in non-degenerate systems, prominently the single harmonic oscillator. One practical example for this issue is intermediate-temperature cavity QED (Rau et al., 2004)

These concepts already found some application in the theoretical literature. We just mention the main results here. After the pioneering work (Governale et al., 2001), it was realized that the high number of rates makes the results difficult to analyze and the performance of quantum gates should be analyzed directly (Thorwart and Hänggi, 2002; Storz and Wilhelm, 2003; Wilhelm et al., 2003). A key result is that (only) the correlated noise model, eq. 102 permits to use symmetries and encoding into decoherence free subspaces to protect coherence (Storz and Wilhelm, 2003; Wilhelm et al., 2003; Storz et al., 2005c), where deviations from perfect symmetry are of relatively low impact (Storz et al., 2005b).

5. Summary

In summary, we have provided an introduction to standard methods in decoherence theory as they are applied to superconducting qubits. Many of the tools and results are more general and can be applied to other damped two-state-systems as well. We see that parts of the theory of decoherence — in particular the part on electromagnetic environments and Bloch-Redfield-Theory — are really well established by now, only opening the view on more subtle problems connected to memory effects and the interplay of decoherence and control.

6. Acknowledgements

This work is based on numerous discussions, too many to list. It is based on our own process of learning and explaining together with other group members, such as M. Goorden, H. Gutmann, A. Käck, A. Holzner, K. Jähne, I. Serban, and J. Ferber. Very importantly, we thank G. Johansson, M. Governale, M. Grifoni, U. Weiss, G. Falci, P. Hänggi, S. Kohler, P. Stamp, L. Tian, S. Lloyd, and H. Gutmann on the theoretical as well as C.H. van der Wal, C.J.P.M. Harmans, J.E. Mooij, T.P. Orlando, J. Clarke, B.L.T. Plourde, and T.L. Robertson on the experimental side. We are very grateful

to M. Flatte and I. Tifrea for organizing the NATO-ASI from which this work originates, and NATO for sponsoring it. Also, the questions of both the participants of the ASI as well as the participants of the course “T VI: Physics of quantum computing” at LMU were very important in identifying the issues asking for explanation. We are deeply indebted to A.G. Fowler for his careful reading of the manuscript and many suggestions helping to make it at least close to pedagogical. This work was supported by the DFG through Sonderforschungsbereich 631, by ARDA and NSA through ARO grant P-43385-PH-QC, and DAAD-NSF travel grants.

References

- Abragam, A. (1983) *Principles of nuclear magnetism*, Vol. 32 of *International series of monographs on physics*, Oxford, Clarendon Press.
- Abramowitz, M. and Stegun, I. (eds.) (1965) *Handbook of mathematical functions*, New York, Dover.
- Argyres, P. and Kelley, P. (1964) Theory of Spin Resonance and Relaxation, *Phys. Rev.* **134**, A98.
- Bertet, P., Chiorescu, I., Burkard, G., Semba, K., Harmans, C., DiVincenzo, D., and Mooij, J. (2005)a Relaxation and Dephasing in a Flux-qubit, *Phys. Rev. Lett.* **95**, 257002.
- Bertet, P., Chiorescu, I., Burkard, G., Semba, K., Harmans, C. J. P. M., DiVincenzo, D. P., and Mooij, J. E. (2005)b Dephasing of a Superconducting Qubit Induced by Photon Noise, *Physical Review Letters* **95**, 257002.
- Blum, K. (1996) *Density Matrix Theory and Applications*, New York, Plenum.
- Brandes, T. and Kramer, B. (1999) Spontaneous emission of phonons by coupled quantum dots, *Phys. Rev. Lett.* **83**, 3021.
- Burkard, G., DiVincenzo, D., Bertet, P., Chiorescu, I., and Mooij, J. E. (2005) Asymmetry and decoherence in a double-layer persistent-current qubit, *Phys. Rev. B* **71**, 134504.
- Caldeira, A. and Leggett, A. (1981) Influence of Dissipation on Quantum Tunneling in Macroscopic Systems, *Phys. Rev. Lett.* **46**, 211.
- Caldeira, A. and Leggett, A. (1983) Quantum tunneling in a dissipative system, *Ann. Phys. (NY)* **149**, 374.
- Callen, H. and Welton, T. (1951) Irreversibility and generalized noise, *Phys. Rev. B* **83**, 34.
- Carr, H. and Purcell, E. (1954) Effects of Diffusion on Free Precession in Nuclear Magnetic Resonance Experiments, *Phys. Rev.* **94**, 630.
- Clarke, J. and Braginski, A. (eds.) (2004) *The SQUID Handbook*, Weinheim, Wiley-VCH.
- Cohen-Tannoudji, C., Diu, B., and Laloë, F. (1992) *Quantum Mechanics*, Weinheim, Wiley Interscience.
- Cottet, A. (2002) Implementation of a quantum bit in a superconducting circuit, Ph.D. thesis, Universite Paris 6.
- de Sousa, R., Whaley, K., Wilhelm, F., and von Delft, J. (2005) Ohmic and Step Noise from a Single Trapping Center Hybridized with a Fermi Sea, *Phys. Rev. Lett.* **95**, 247006.
- Dutta, P. and Horn, P. (1981) Low-frequency fluctuations in solids: 1/f-noise, *Rev. Mod. Phys.* **53**, 497.

- Falci, G., D'Arrigo, A., Mastellone, A., and Paladino, E. (2004) Dynamical suppression of telegraph and $1/f$ noise due to quantum bistable fluctuator, *Phys. Rev. A* **70**, R40101.
- Faoro, L., Bergli, J., Altshuler, B. L., and Galperin, Y. M. (2005) Models of Environment and T₁ Relaxation in Josephson Charge Qubits, *Physical Review Letters* **95**, 046805.
- Faoro, L. and Viola, L. (2004) Dynamical suppression of $1/f$ noise processes in qubit systems, *Phys. Rev. Lett.* **92**, 117905.
- Feynman, R. and Vernon, F. (1963) The theory of a general quantum system interacting with a linear dissipative system, *Ann. Phys. (N.Y.)* **24**, 118.
- Galperin, Y., Altshuler, B., and Shantsev, D. (2003) *Fundamental problems of mesoscopic physics: Interaction and decoherence*, Chapt. Low-frequency noise as a source of dephasing a qubit, NATO-ASI, New York, , Plenum.
- Geller, M., Pritchett, E., and Sornborger, A. (2006) *Manipulating quantum coherence in semiconductors and superconductors*, Chapt. Quantum computing with superconductors: architectures, New York, , Springer, edited by M. Flatte and I. Tifrea.
- Giulini, D., Joos, E., Kiefer, C., Kupsch, J., Stamatescu, I.-O., and Zeh, H. D. (1996) *Decoherence and the Appearance of a Classical World in Quantum Theory*, Heidelberg, Springer.
- Goorden, M. and Wilhelm, F. (2003) Theoretical analysis of continuously driven solid-state qubits, *Phys. Rev. B* **68**, 012508.
- Görlich, R. and Weiss, U. (1988) Specific heat of the dissipative two-state system, *Phys. Rev. B* **38**, 5245.
- Governale, M., Grifoni, M., and Schön, G. (2001) Decoherence and dephasing in coupled Josephson-junction qubits, *Chem. Phys.* **268**, 273.
- Grishin, A., Yurkevich, I. V., and Lerner, I. V. (2005) Low-temperature decoherence of qubit coupled to background charges, *Physical Review B (Condensed Matter and Materials Physics)* **72**, 060509.
- Gutmann, H., Kaminsky, W., Lloyd, S., and Wilhelm, F. (2005) Compensation of decoherence from telegraph noise by means of an open loop quantum-control technique, *Phys. Rev. A* **71**, 020302(R).
- Gutmann, H. and Wilhelm, F. (2006) Complete positivity for certain low-temperature master equations, in preparation.
- Harlingen, D. J. V., Robertson, T. L., Plourde, B. L., Reichardt, P., Crane, T., and Clarke, J. (1988) Decoherence in Josephson-junction qubits due to critical-current fluctuations, *Phys. Rev. B* **70**, 064517.
- Hartmann, L., Goychuk, I., Grifoni, M., and Hanggi, P. (2000) Driven tunneling dynamics: Bloch-Redfield theory versus path-integral approach, *Physical Review E (Statistical Physics, Plasmas, Fluids, and Related Interdisciplinary Topics)* **61**, R4687–R4690.
- Hartmann, U. and Wilhelm, F. (2004) Control of decoherence through nonequilibrium between two baths, *Phys. Rev. B* **69**, 161309(R).
- Ingold, G. (1998) *Quantum transport and dissipation*, Chapt. Dissipative quantum systems, Weinheim, , Wiley-VCH.
- Ioffe, L., Geshkenbein, V., Helm, C., and Blatter, G. (2004) Decoherence in Superconducting Quantum Bits by Phonon Radiation, *Phys. Rev. Lett.* **93**, 057001.
- Kehrein, S. and Mielke, A. (1998) Diagonalization of system plus environment Hamiltonians, *J. Stat. Phys.* **90**, 889.

- Kubo, R., oda, M., and Hashitsume, N. (1991) *Statistical Physics II*, Vol. 31 of *Springer series in solid-state statistical physics*, Tokyo, Springer.
- Landau, L. and Lifshitz, E. (1982) *Mechanics*, Vol. 1 of *Course of Theoretical Physics*, Burlington, MA, Butterworth-Heinemann.
- Landau, L. and Lifshitz, E. (1984) *Statistical Physics*, Vol. 5 of *Course of Theoretical Physics*, Burlington, MA, Butterworth-Heinemann.
- Leggett, A. (2002) Testing the limits of quantum mechanics: Motivation, state of play, and prospects, *J. Phys. C* **14**, 415.
- Leggett, A., Chakravarty, S., Dorsey, A., Fisher, M., Garg, A., and Zwerger, W. (1987) Dynamics of the dissipative two-state system, *Rev. Mod. Phys.* **59**, 1.
- Lidar, D., Shabani, A., and Alicki, R. (2004) Conditions for strictly purity-decreasing quantum Markovian dynamics, quant-ph/0411119.
- Lindblad, G. (1976) On the generators of quantum dynamical semigroups, *Commun. Math. Phys.* **48**, 119.
- Loss, D. and DiVincenzo, D. (2003) Exact Born Approximation for the Spin-Boson Model, cond-mat/0304118.
- Lupascu, A., Verwijs, C., Schouten, R. N., Harmans, C., and Mooij, J. E. (2004) Nondestructive Readout for a Superconducting Flux Qubit, *Phys. Rev. Lett.* **93**, 177006.
- Mahan, G. (2000) *Many Particle Physics*, New York, Springer.
- Makhlin, Y., Schön, G., and Shnirman, A. (2001) Quantum-state engineering with Josephson-junction devices, *Rev. Mod. Phys.* **73**, 357.
- Martinis, J., Nam, S., Aumentado, J., Lang, K., and Urbina, C. (2003) Decoherence of a superconducting qubit due to bias noise, *Phys. Rev. B* **67**, 094510.
- Nakajima, S. (1958) On Quantum Theory of Transport Phenomena - Steady Diffusion, *Prog. Theor. Phys.* **20**, 948.
- Paladino, E., Faoro, L., Falci, G., and Fazio, R. (2002) Decoherence and 1/f noise in Josephson qubits, *Phys. Rev. Lett.* **88**, 228304.
- Peres, A. (1993) *Quantum Theory: Concept and Methods*, Dordrecht, Kluwer.
- Rau, I., Johansson, G., and Shnirman, A. (2004) Cavity quantum electrodynamics in superconducting circuits: Susceptibility at elevated temperatures, *Physical Review B (Condensed Matter and Materials Physics)* **70**, 054521.
- Robertson, T. L., Plourde, B. L. T., Hime, T., Linzen, S., Reichardt, P. A., Wilhelm, F. K., and Clarke, J. (2005) Superconducting quantum interference device with frequency-dependent damping: Readout of flux qubits, *Physical Review B (Condensed Matter and Materials Physics)* **72**, 024513.
- Sakurai, J. (1967) *Advanced Quantum Mechanics*, New York, Addison-Wesley.
- Schleich, W. (2001) *Quantum Optics in Phase Space*, Weinheim, Wiley-VCH.
- Schrödinger, E. (1935) Die gegenwärtige Situation in der Quantenmechanik, *Naturwissenschaften* **23**, 807, 823, 844.
- Shiokawa, K. and Lidar, D. A. (2004) Dynamical decoupling using slow pulses: Efficient suppression of 1/f noise, *Physical Review A (Atomic, Molecular, and Optical Physics)* **69**, 030302.
- Shnirman, A., Makhlin, Y., and Schön, G. (2002) Noise and decoherence in quantum two-level systems, *Phys. Scr.* **T102**, 147.
- Shnirman, A., Schon, G., Martin, I., and Makhlin, Y. (2005) Low- and High-Frequency Noise from Coherent Two-Level Systems, *Physical Review Letters* **94**, 127002.
- Simmonds, R., Lang, K., Hite, D., Pappas, D., and Martinis, J. (2004) Decoherence in Josephson Qubits from Junction Resonances, *Phys. Rev. Lett.* **93**, 077003.

- Storcz, M. and Wilhelm, F. (2003) Decoherence and gate performance of coupled solid-state qubits, *Phys. Rev. A* **67**, 042319.
- Storcz, M. J., Hartmann, U., Kohler, S., and Wilhelm, F. K. (2005)a Intrinsic phonon decoherence and quantum gates in coupled lateral quantum-dot charge qubits, *Physical Review B (Condensed Matter and Materials Physics)* **72**, 235321.
- Storcz, M. J., Hellmann, F., Hrelescu, C., and Wilhelm, F. K. (2005)b Decoherence of a two-qubit system away from perfect symmetry, *Physical Review A (Atomic, Molecular, and Optical Physics)* **72**, 052314.
- Storcz, M. J., Vala, J., Brown, K. R., Kempe, J., Wilhelm, F. K., and Whaley, K. B. (2005)c Full protection of superconducting qubit systems from coupling errors, *Physical Review B (Condensed Matter and Materials Physics)* **72**, 064511.
- Thorwart, M., Eckel, J., and Mucciolo, E. (2005) Non-Markovian dynamics of double quantum dot charge qubits due to acoustic phonons, *Phys. Rev. B* **72**, 235320.
- Thorwart, M. and Hänggi, P. (2002) Decoherence and dissipation during a quantum XOR gate operation, *Phys. Rev. A* **65**, 012309.
- Tinkham, M. (1996) *Introduction to Superconductivity*, New York, McGraw-Hill.
- van der Wal, C., Wilhelm, F., Harmans, C., and Mooij, J. (2003) Engineering decoherence in Josephson persistent-current qubits, *Eur. Phys. J. B* **31**, 111.
- van Kampen, N. (1997) *Stochastic processes in physics and chemistry*, Amsterdam, Elsevier.
- Vion, D., Aassime, A., Cottet, A., Joyez, P., Pothier, H., Urbina, C., Esteve, D., and Devoret, M. (2002) Manipulating the quantum state of an electrical circuit, *Science* **296**, 286.
- von Delft, J. and Schoeller, H. (1998) Bosonization for Beginners - Refermionization for Experts, *Ann. Phys. (Leipzig)* **7**, 225.
- Wakai, R. and van Harlingen, D. (1987) Direct lifetime measurements and interactions of charged defect states in submicron Josephson junctions, *Phys. Rev. Lett.* **58**, 1687.
- Wallraff, A., Schuster, D., Blais, A., Frunzio, L., Majer, J., Girvin, S., and Schoelkopf, R. J. (2005) Approaching Unit Visibility for Control of a Superconducting Qubit with Dispersive Readout, cond-mat/0502645.
- Walls, D. and Milburn, G. (1994) *Quantum Optics*, Berlin, Springer.
- Weiss, U. (1999) *Quantum Dissipative Systems*, No. 10 in Series in modern condensed matter physics, Singapore, World Scientific, 2 edition.
- Weissman, M. (1988) $1/f$ noise and other slow, nonexponential kinetics in condensed matter, *Rev. Mod. Phys.* **60**, 537.
- Wilhelm, F. (2003) Reduced visibility in the spin-Boson model, cond-mat/0507026.
- Wilhelm, F., Storcz, M., van der Wal, C., Harmans, C., and Mooij, J. (2003) Decoherence of flux qubits coupled to electronic circuits, *Adv. Sol. St. Phys.* **43**, 763.
- Zill, D. (2000) *A first course in differential equations*, Florence, KY, Brooks Cole.
- Zurek, W. (1993) Preferred States, Predictability, Classicality and the Environment-Induced Decoherence, *Prog. Theor. Phys.* **89**, 281.
- Zwanzig, R. (1960) Ensemble method in the theory of irreversibility, *J. Chem. Phys.* **33**, 1338.